GLASS (AND GLASS-CERAMICS) FOR BATTERIES

Virginie VIALLET

LRCS - Hub de l'énergie (Amiens)
Université Picardie Jules Verne

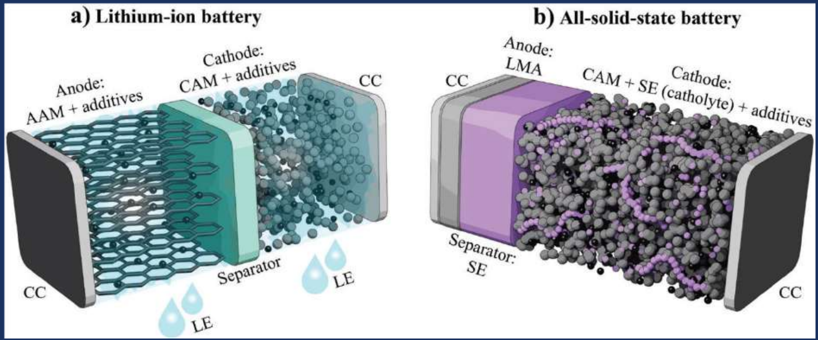

Glass for a sustainable future
April 29 – May 03, 2024, Lloret del Mar, Spain

Amiens city

140 km north of Paris

LRCS - Hub de l'énergie (Amiens)
Université Picardie Jules Verne

UMR (Mixed Research Unit)

Hub de l'énergie

National Network RS2E : Network on Electrochemical Energy Storage

17 research laboratories

15 industrial partners

3 public establishments of an industrial and commercial nature

TOTAL = 136 persons

42 Permanents

75 non-permanents
+ 19 companies

G+LYTE

TIAMAT

LRCS – HUB of Energy

Institut Charles Gerhardt Montpellier

Batteries

Lithium-Ion Batteries

Organic Batteries

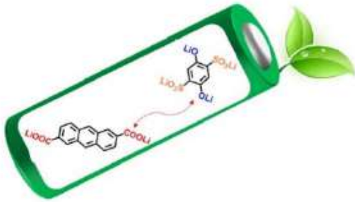

Sodium-Ion Batteries

Redox-Flow Batteries

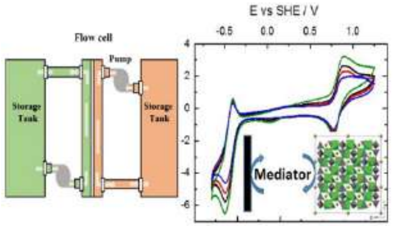

Lithium-Sulfur Batteries

All Solid State Batteries

Glasses and Glass-Ceramics for Solid-State Battery Applications

Virginie Viallet, Vincent Seznec, Akitoshi Hayashi, Masahiro Tatsumisago, Annie Pradel

Pages 1697-1754

Metal-Air Batteries

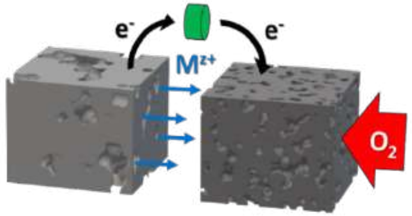

Glass and Glass-ceramic
Collaborations
Annie Pradel
Andrea Piarristeguy

Hydrogen Storage

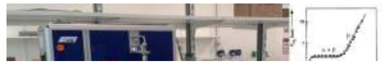

Photovoltaic Devices

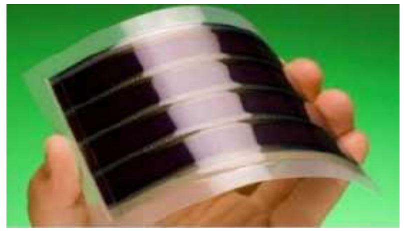

LRCS - Exploration of the full chain of the design technologies processes

LRCS

Synthesis of inorganic materials

Organic, hybrid and polymer materials for energy

Structural studies

development of new investigative tools

electrochemistry and development of new devices for electrochemical storage

Photoelectrochemistry and photovoltaic devices

G+LYTE

pre-transfer platform materials prototyping safety

TIAMAT

modeling: from material to electrochemical system

1/Playing with the materials synthesis methods

2/Understanding of the structure/properties relationships of the materials

3/Testing the material performances in laboratory cells

4/Industrial technology transfer with modeling and prototyping

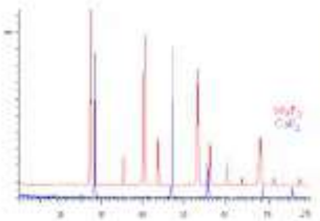

OUTLINE

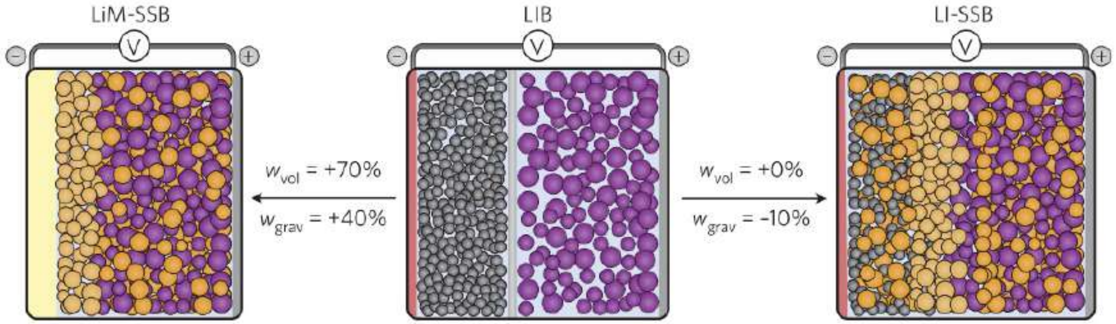

1

Batteries: from liquid to solid electrolyte

1.1. Batteries for renewable energy storage
1.2. Limitations of traditional Li-ion batteries
1.3. Advantages and challenges of All-Solid-State Batteries (ASSB)

- Increased in world population

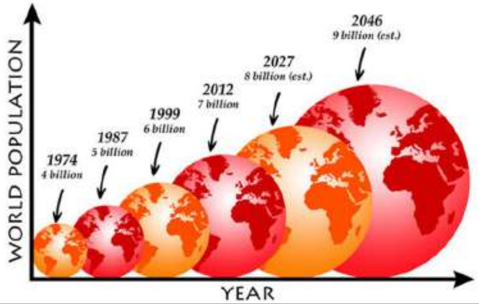

- Increased energy needs

World primary energy consumption by source

(Source: Energy Institute Statistical Review of World Energy 2023)

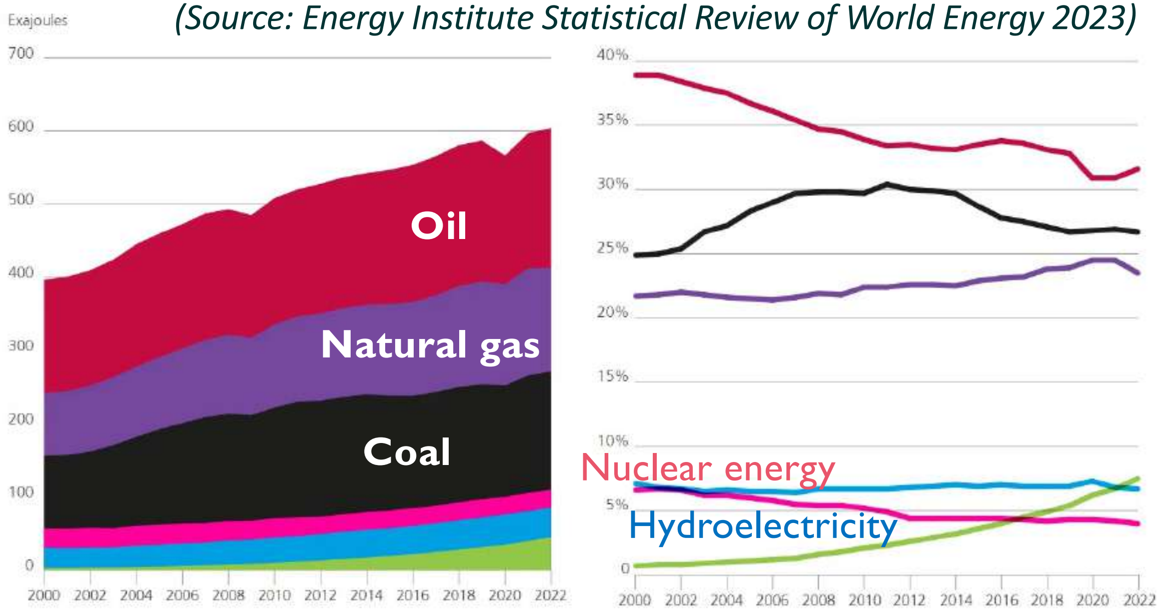

fossil fuels dominate

Renewables
include solar, wind, geothermal, biomass, and waste

Exponential increase in primary energy production to meet demand

In 2021, 82% of the energy consumed worldwide come from fossil fuels measurements CO_2 emission over the last 120 years

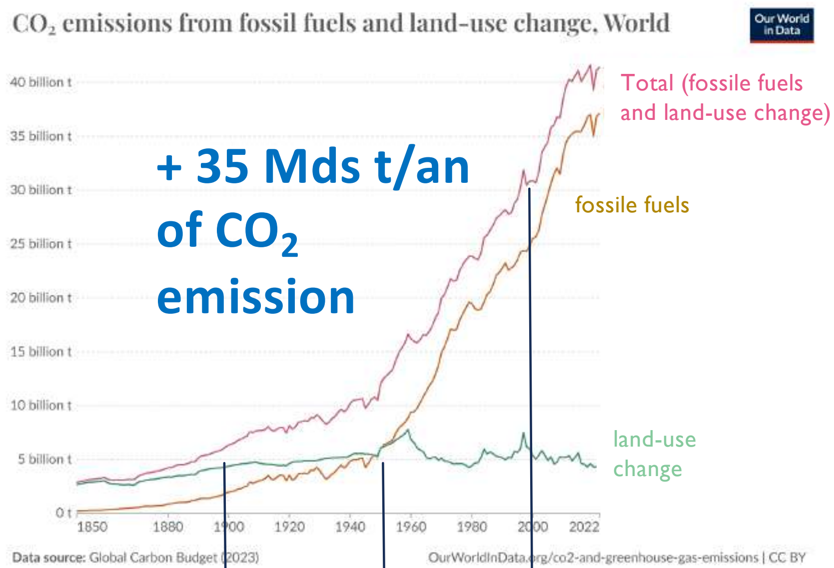

measurements of temperatures and CO_2 emissions

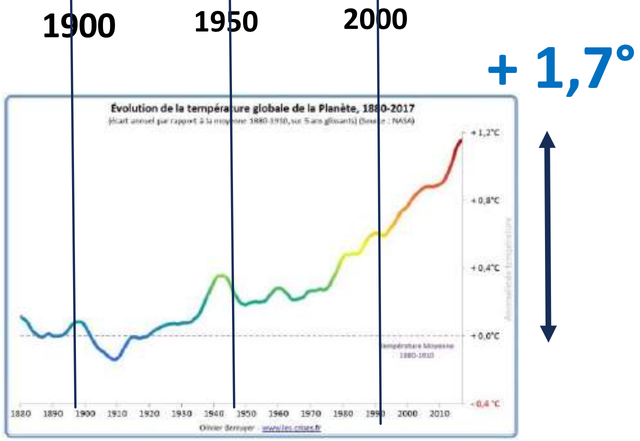

massive consumption of fossil fuels is contributing to global warming.

Depletion of fossil energy resources

Development of renewable energies
Storage

Lithium-ion batteries are one of the favoured options for renewable energy storage.
They are widely seen as one of the main solutions to compensate for the intermittency of wind and sun energy.

Li-ion battery ($LiCoO_2$ – graphite) SONY 1991

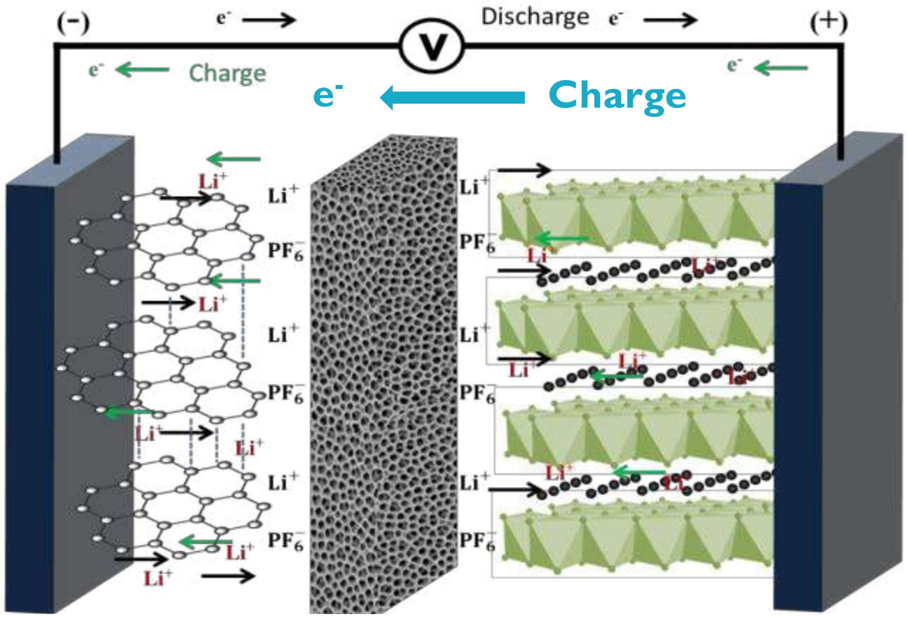

graphite
372 mAh.g^{-1}

Porous separator

$LiCoO_2$
135 mAh.g^{-1}

Aprotic liquid electrolyte LiPF6 salt dissolved in a mixture of ethylene carbonate (EC), propylene carbonate (PC) or tetrahydrofuran ($(CH_2)_4O$)

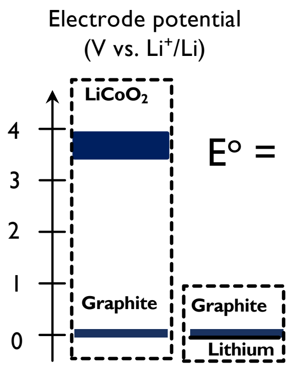

E° = ~ 3,7 V

Capacity C (A.h)

$$C = \frac{F.x}{3600.M} = \frac{96485.x}{3600.M}$$

$C_{cathode}(LiCoO_2)_{theo}$ = 135 mAh.g^{-1}

$C_{anode}(C_6)_{theo} = \frac{96485.1}{3600.(6\times12)} =$
= 372 mAh.g^{-1}

Energy

$$E = \frac{C_c \times C_a}{C_c + C_a} \times V_{cell}$$

Power

$P = V_{cell} \times I$

260 Wh.Kg^{-1}

Limitation

Charge

Negative electrode
$C_6 + n\,Li^+ + ne^- \rightarrow Li_nC_6$

Positive Electrode
$LiCoO_2 \rightarrow Li_{1-n}CoO_2 + n\,Li^+ + ne^-$

Reaction : $LiCoO_2 + C_6 = Li_nC_6 + Li_{1-n}CoO_2$, E° = ~ 3,7 V

positive electrode materials

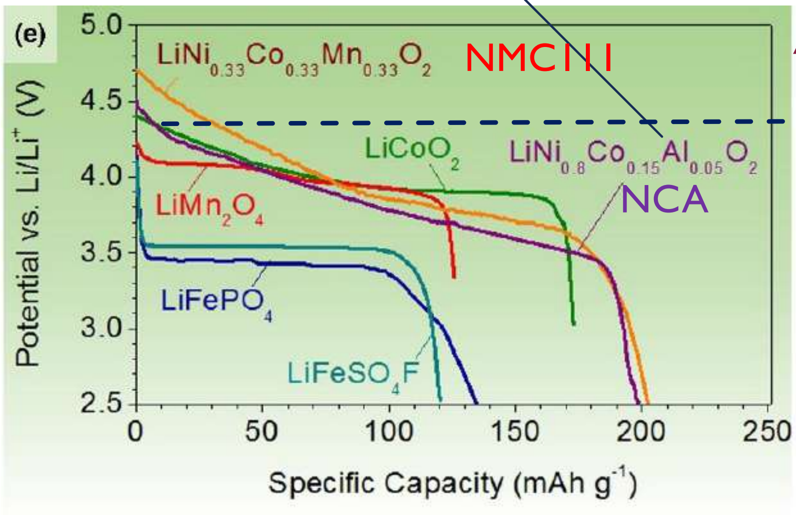

high-energy cathode material

$LiCoPO_4$ 4.8 V *vs.* Li/Li^+ ~801 Wh kg^{-1}

$LiNi_{0.5}Mn_{1.5}O_4$ 4.7 V *vs.* Li/Li^+ ~690 Wh kg^{-1}

Stability window
Solid electrolyte?

Stability window
liquid electrolyte

Energy density increase

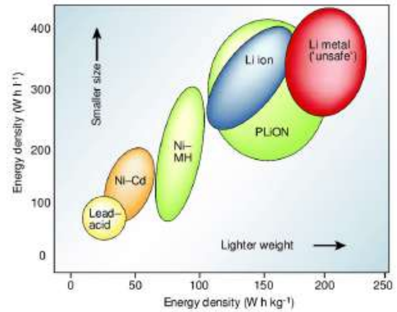

Energy density
= capacity x potential

volumetric and gravimetric energy densities (W_{vol}, W_{grav})

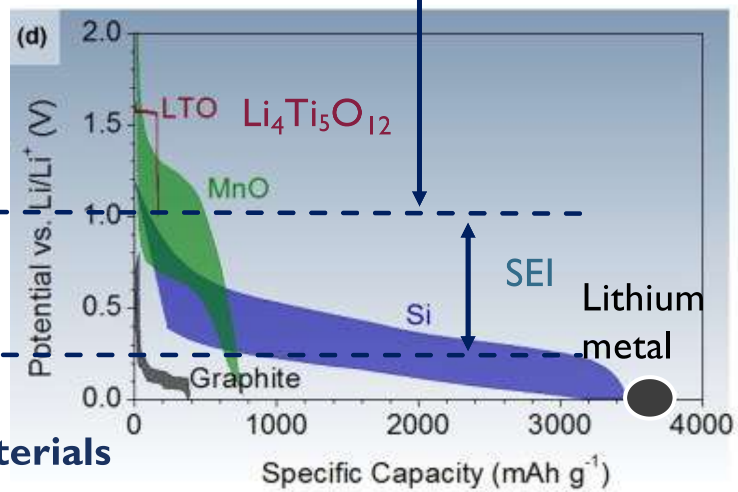

lithium (Li) metal

- high theoretical specific capacity (3860 mAh g^{-1}),
- low density (0.59 g cm^{-3})
- and the lowest negative electrochemical potential

⇒ ideal negative electrode for the high energy density rechargeable batteries

negative electrode materials

positive electrode materials

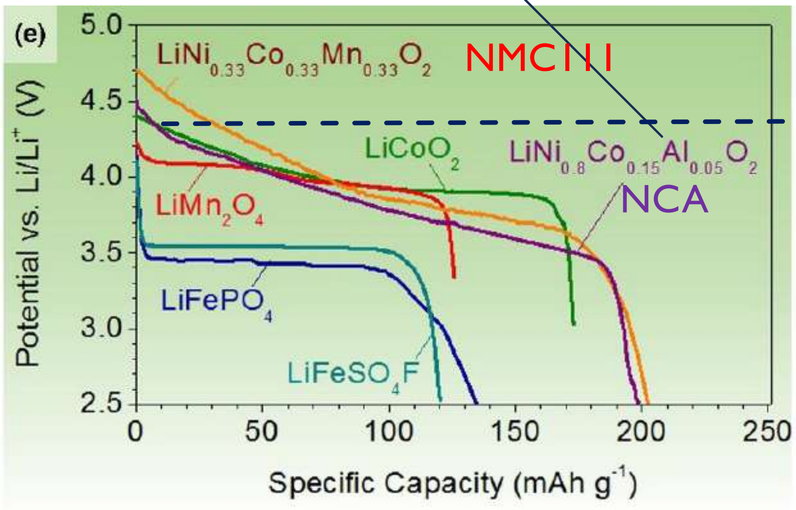

high-energy cathode material

$LiCoPO_4$	4.8 V *vs.* Li/Li^+	~801 Wh kg^{-1}
$LiNi_{0.5}Mn_{1.5}O_4$	4.7 V *vs.* Li/Li^+	~690 Wh kg^{-1}

Poster 6 (Guyot Taos) - Cathode properties of Iron Based Oxide Glasses for Sustainable and High-Energy Density Lithium-ion Batteries

Glassy Cathode:

- Wide range of chemical compositions
- Accommodation of structural changes upon lithium ions extraction and insertion
- Glass production scalable and commercially easier to implement

Energy density increase

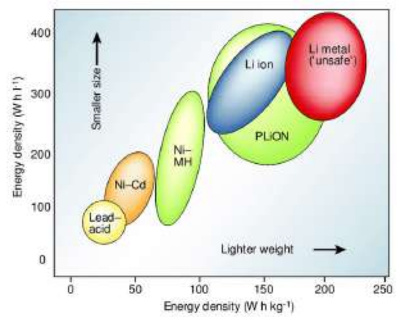

Energy density
= capacity x potential

volumetric and gravimetric energy densities (W_{vol}, W_{grav})

Current manufactured batteries still face issues:
Flammable organic solvent

Deformation and ignition due to overheating.
- Leakage of liquid electrolyte.
- Limitation of Voltage

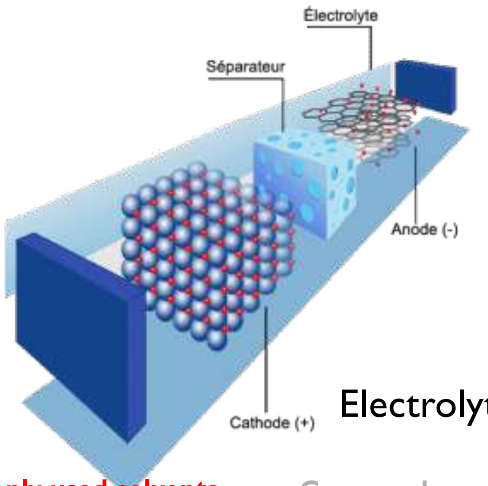

Electrolyte

Commonly used solvents

Linear Solvents :
- Diethyl Carbonate (DEC)
- Dimethyl Carbonate (DMC)
- Ethyl Methyl Carbonate (EMC)

Cyclic Solvents :
- Ethylene Carbonate (EC)
- Propylene Carbonate (PC)
- Butylene Carbonate (BC)
- γ– butyrolactone (GBL)

Commonly used salts

- Li hexafluorophosphate ($LiPF_6$)
- Li fluroroborate ($LiBF_4$)
- Li Perchlorate ($LiClO_4$)
- Li hexafluoroarsenate ($LiAsF_6$)

Dell, Apple batteries Sony
oct. 2006

TESLA Car: LFP/Graphite
USA, oct. 2013

Dreamliner Boeing 787
january 2013,
(Boston, Japon)

High risk above 60 °C

Extremely narrow operating temperature range 15-45 °C

-Electrolytes could break down into flammable gases
- Toxic gases (HF)
-Separators could melt, possibly causing a short circuit

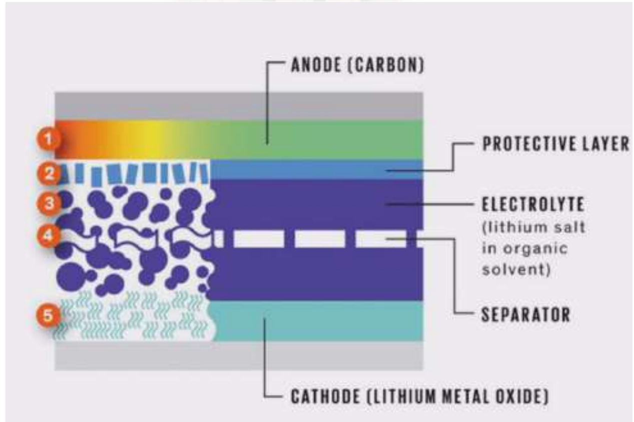

Journal of Power Sources (2018) 400:621-640

Pros…

Energy density increase

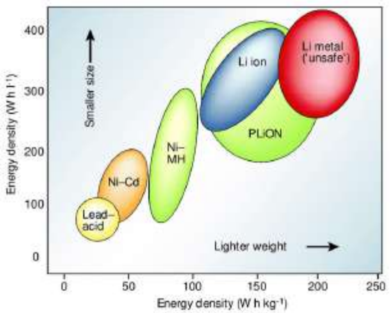

Energy density
= capacity x potential

volumetric and gravimetric energy densities (W_{vol}, W_{grav})

$$C(Li_{metal})_{theo} = \frac{96485 \times 1}{3600 \times (6.94)} = 3862 \text{ mAh.g}^{-1}$$

Solid state battery with a lithium-metal anode

Conventional lithium-ion batteries

Lithium ion all-solid-state battery with a conventional anode

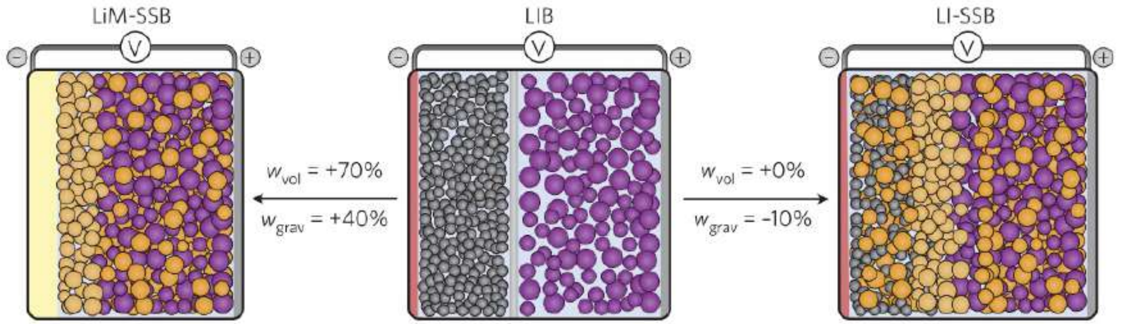

Cu collector Al collector

Safety issues

Package down-sizing: EV

No more separator

Reduced battery weights

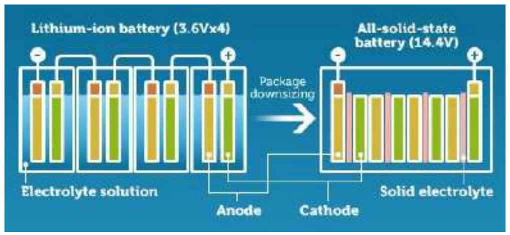

https://www.toyota.com.bh/about/technology/environmental-technology/next-generation-secondary-batteries/

Reduced cost

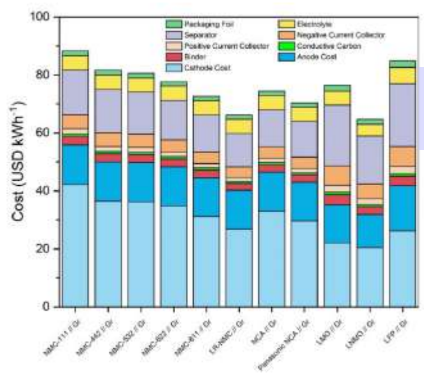

Thin separator

https://thedeepdive.ca/lithium-ion-battery-cells-cathodes-and-costs/ February 2019

High temperatures application

Desert Environments

Automotive Windshields

drilling station batteries

Solid electrolyte

Ranking of properties of solid electrolytes (5 = best, 1 = worst).

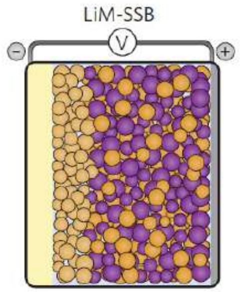

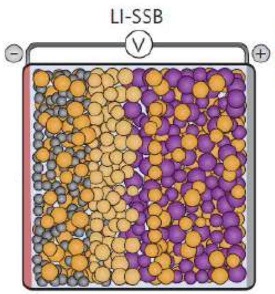

Low $\sigma_{electron} < 10^{-12}$ S.cm^{-1}

$\sigma_{ion} \geq 10^{-4}$ S.cm^{-1}

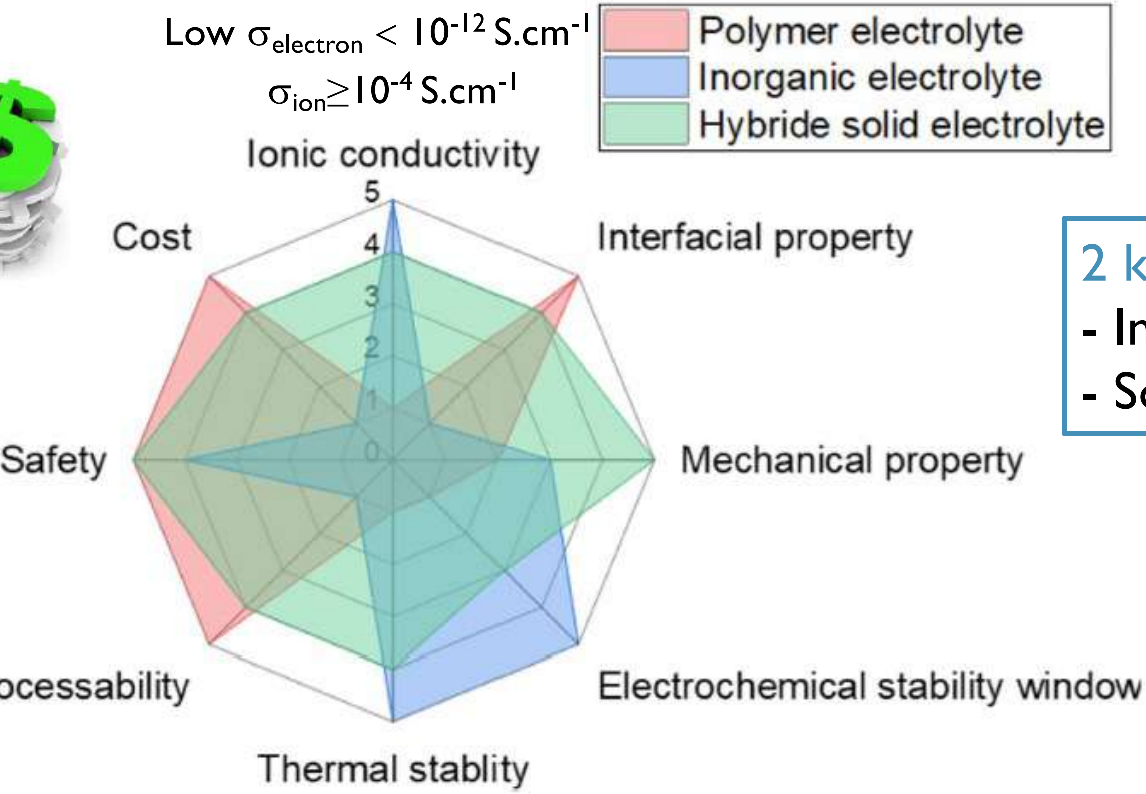

2 key points:
- Interfaces optimization
- Solid electrolyte

L. Han *et al*, Frontiers in energy research, Vol. 8, article 202, 2020

Solid state battery with a lithium-metal anode

Pros… And Cons…

2 key points:
- Interfaces optimization
- Solid electrolyte

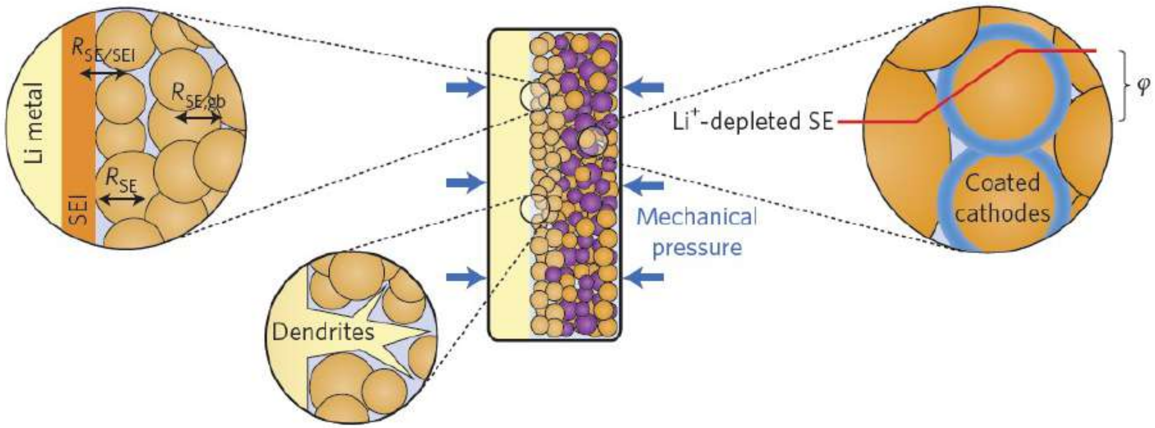

process of industrialization is still limited by technological, marketing and financial factors.

On the technological side, the research of SSE synthesis method, stability, conductivity and interfacial properties is the key to practical application.

electric resistance between electrolytes and electrode materials is large because of the limited contact area
⇒ solid composite electrodes ensuring sufficient electronic and ionic percolation have to be formed

J. Janek & W. G. Zeier, Nature Energy, Vol. 1, 2016

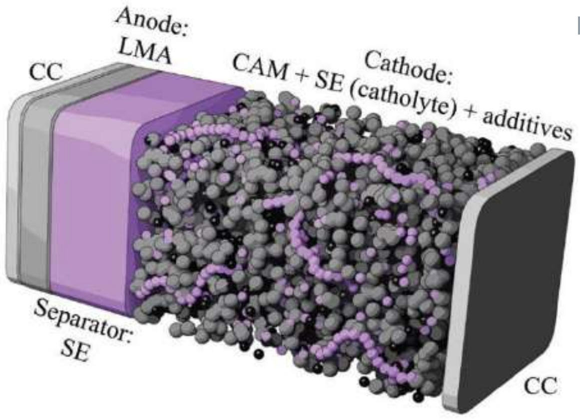

2 Glasses and glass-ceramics for Li-ion ASSB

2.1. Solid electrolytes (SE)

Oxides

Sulfides

2.2. All-Solid-State Batteries (ASSB)

Which ionic conductors?

Inorganic solids
- **Crystalline phases,**
- **Glass,**
- **or Glass-ceramics**

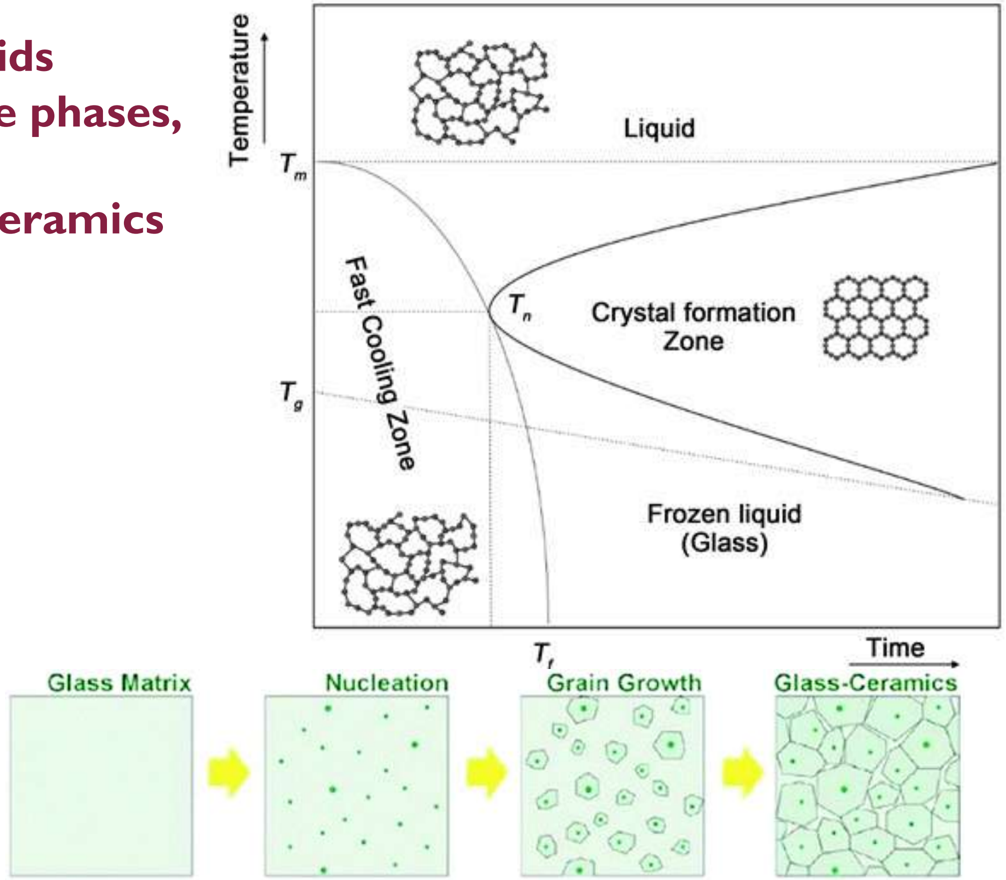

Ali S. Alzahrani
Advances in Materials Physics and Chemistry, 2022, 12, 261-288

Organic Solid Polymers

Solid Polymer Electrolytes (SPE)

Gel Polymer Electrolytes (GPE)

80 °C to operate (BlueCar)

Composite Solid Electrolyte Polymers and inorganic…

S. Liu et al, J. Mater. Chem. C, 2019, 7, 15118-15135

2,184 Publications for: conducting & glass & glass-ceramic electrolyte*
623 results for: glass and glass ceramic all solid state batteries

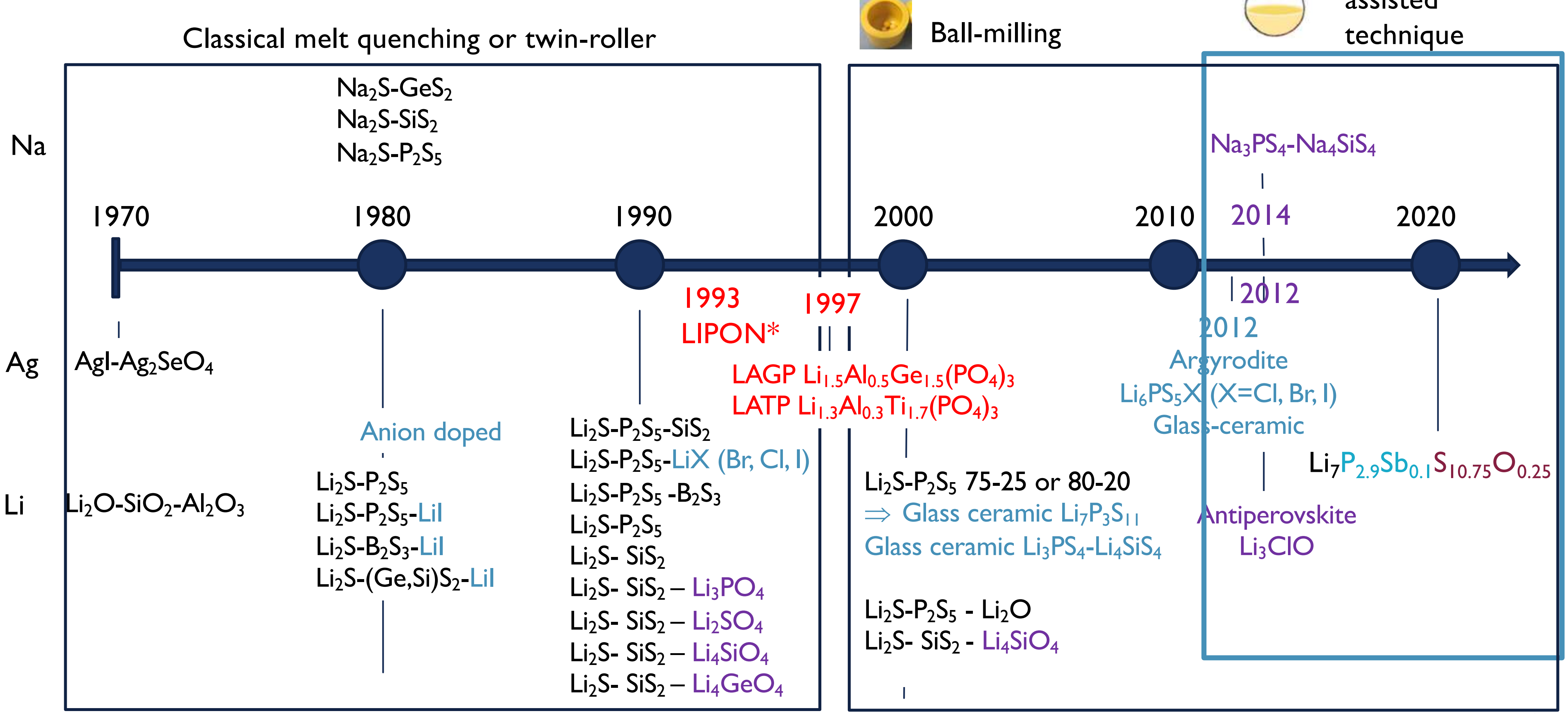

* microbatteries
*results from Web of Science Core Collection (Topic)

Glass or glass-ceramic formation

1970 — 1980 — 1990 — 2000 — 2010 — 2020

Classical routes
From the 1970s to 2000

New synthetic routes
Since the 2000s

Melting
+ quenching

thermal-image furnace
and twin roller

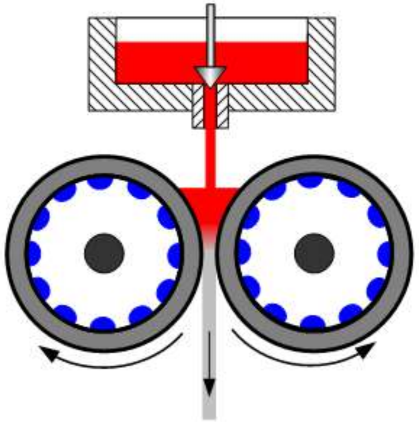

Ball-milling (BM)
Or Mechanicall Milling

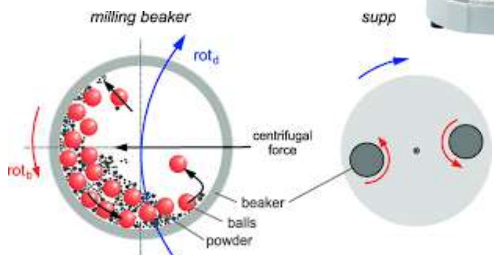

Nature of the balls and pots
Speed
Duration of milling
…

Solvent assisted synthesis

Scale-up

Compatibility
with battery
fabrication
process

Two main types

Inorganic solids
(crystalline, glass or glass-ceramics)

Oxides and phosphates

- Handling under room atmosphere

- Brittle
and often experience mechanical failure through cracking
- Sintering at high temperature

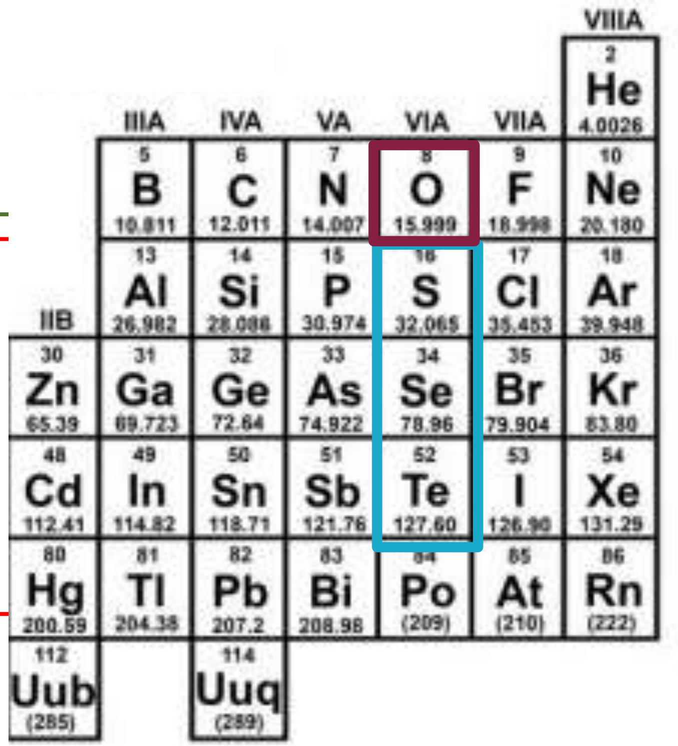

Chalcogenides
Mostly sulfides
Intensively studied

- Sulfides are ductile
- easily form dense cathode and anode composites

- But moisture sensitive:
partial hydrolysis & H_2S toxic gas formation
⇒ Ionic conductivity drop
⇒ Safety problems

interest of glasses compared to crystallized phases

glass

polycrystalline ceramic

For polycrystalline ceramic SSEs, the Li^+ transport mechanism depends on three factors:
-carrier type,
- diffusion pathways and
- diffusion type.

The carrier type and concentration are determined by the point defects in the polycrystalline ceramic structure, which directly affect the ionic conductivity.

The interactions between Li ions during migration in the crystal and between ones and the surrounding environment will significantly affect the ionic conductivity.

Compared to ceramic SSEs, amorphous (glass) SSEs:
- have better flexibility, uniformity and density.
- show no grain boundary resistance and isotropic Li^+ mobility.

These properties of glass SSEs have prompted attempts to find its ionic conduction mechanism.
At present, although many experimental data on Li^+ conduction in glass SSEs are available, the Li^+ conduction mechanism in glass SSEs is still not well explained, and no relevant general theory has been established.

Casasola, R., Rincón, J. M., & Romero, M. (2012). Glass–ceramic glazes for ceramic tiles: a review. Journal of Materials Science, 47, 553-582.

interest of glasses compared to crystallized phases

Glass

- Wide selection of composition
  (100-x)Li_2S-xP_2S_5
  Li_2S-P_2S_5- LiI
  Li_2S-SiS_2
- Non flammability
- Easy film formation
- Ionic conductivity generally > Ionic conductivity crystal
- Single cation conduction
  Li^+ conducting glasses
  Na^+ conducting glasses

Heating of the glass

- Stable crystalline phase with lower Grain-Boundary resistance
  LATP and LAGP
- Glass-ceramics
  80-20 Li_2S-P_2S_5
  70-30 Li_2S-P_2S_5
  $Li_7P_3S_{11}$
- Superionic conductive crystal
  $Li_7P_3S_{11}$
  Na_3PS_4

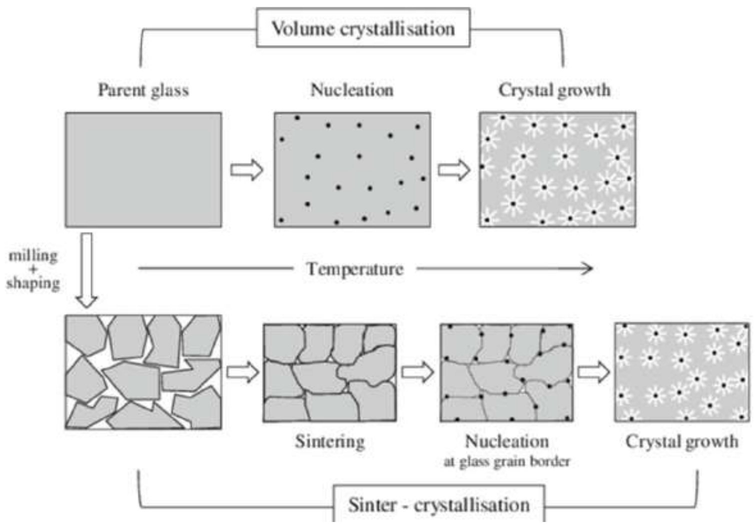

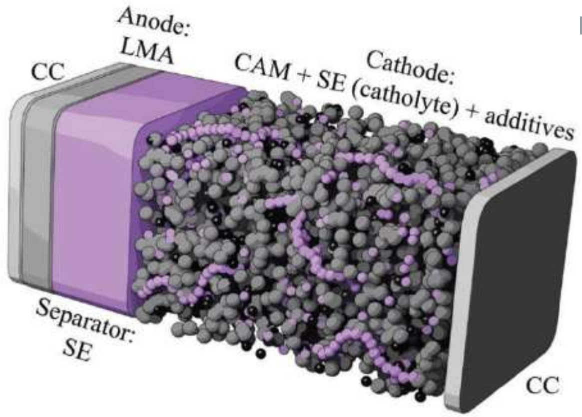

2 Glasses and glass-ceramics for Li-ion ASSB

2.1. Solid electrolytes (SE)

Oxides

Sulfides

2.2. All-Solid-State Batteries (ASSB)

Oxide Glass and Glass ceramic systems

From ceramic...

Most of the oxide SSEs are polycrystalline ceramic SSEs whose advantages are:

- high ionic conductivity,
- high mechanical strength and
- a wide electrochemical stability window.

However, the interface problem between this type of SSEs and electrodes is more prominent.

garnet-type Li-ion electrolytes based on cubic $\mathbf{Li_7La_3Zr_2O_{12}}$ **(LLZO)** most appealing candidate

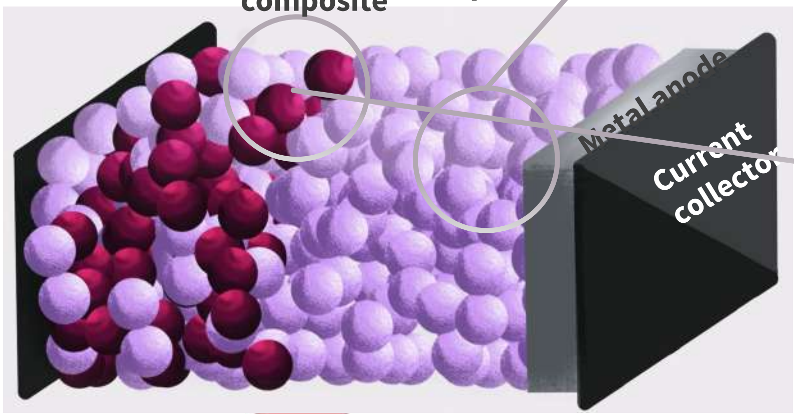

Interfacial Issues in ASSB

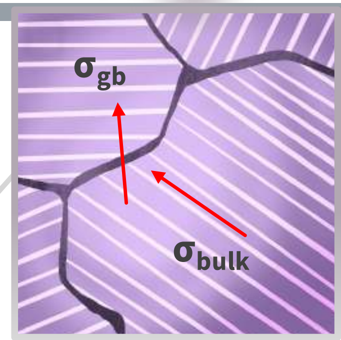

Grain boundary formation
Between SEs particles or SEs-Active material

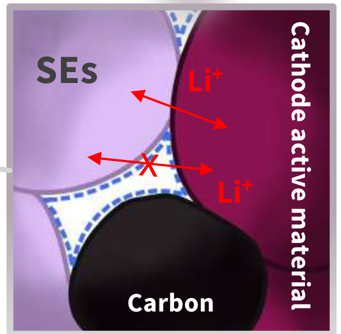

Void and contact issues
Increased resistance and volume

Oxide Glass and Glass ceramic systems

From ceramic…

Most of the oxide SSEs are polycrystalline ceramic SSEs whose advantages are:

- high ionic conductivity,
- high mechanical strength and
- a wide electrochemical stability window.

However, the interface problem between this type of SSEs and electrodes is more prominent.

to glass and glass ceramic

advantages in terms of:
-flexibility,
-homogeneity and
- density.

Therefore, glass-ceramic SSEs are prepared by melting-quenching and partial crystallization of glass, which not only improve the ionic conductivity but also optimize the interface between SSEs and electrodes to some extent.

Oxide Glass and Glass ceramic systems

No glass used in All-Solid-State Batteries

Only Glass-ceramics

Lithium analogues of NASICON-type compounds
are heavily investigated as promising SSEs for ASSLIBs

Melt quenching method

(1) Mixture of raw materials melted at high temperatures
(2) Rapid cooling to form the parent glass
(3) Annealing to release stress
(4) Heat treatment to nucleate and grow NASICON crystals in the glass (nucleation agents often added)
(5) Mechanical Ball Milling to obtain nano-size glass or glass ceramic material

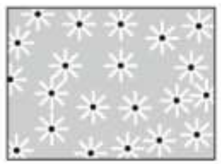

Mainly Two NASICON-type compounds studied

LATP $Li_{1.3}Al_{0.3}Ti_{1.7}(PO_4)_3$

LGTP $Li_{1.5}Ge_{0.5}Ti_{1.5}(PO_4)_3$

NASICON structure

$NaM_2(PO_4)_3$ [M^{4+}], e.g., Ge, Ti, Sn and Zr.
$Na_{1+x}Zr_2Si_xP_{3-x}O_{12}$ ($0 < x < 3$) NASICON

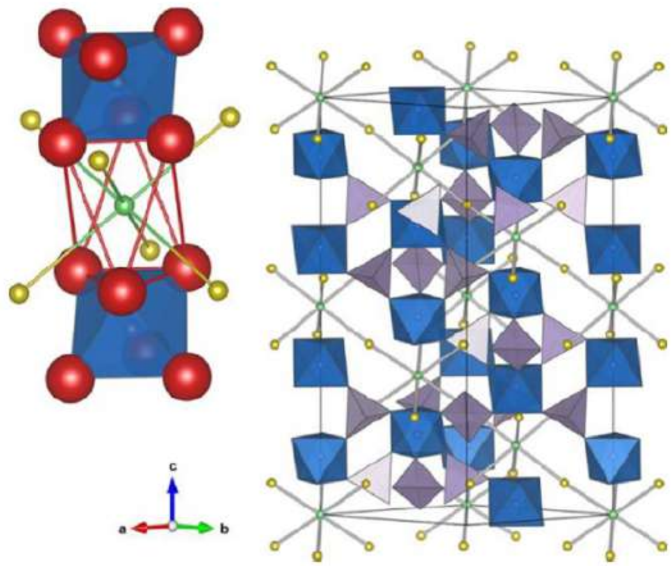

Blue octahedra are MO_6 units, Purple tetrahedra are PO_4 units, green spheres are M1 sites and yellow spheres are M2 sites

Stable crystalline phase with lower Grain-Boundary resistance

$Li_{1.5}Al_{0.5}Ti_{1.5}(PO_4)_3$ $\sigma_{glass\text{-}ceramic}$ about 1×10^{-4} Scm^{-1} > $\sigma_{ceramic}$ 6×10^{-5} Scm^{-1} > σ_{glass} 10^{-10} - 10^{-8} Scm^{-1}

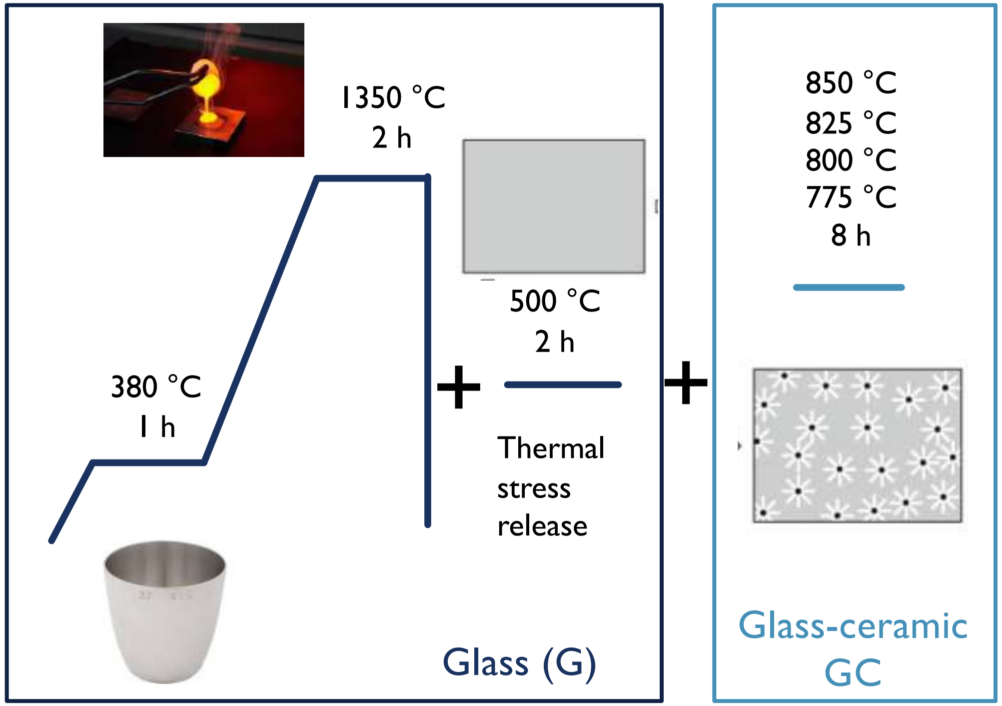

Li_2CO_3 + Al_2O_3 + TiO_2 + $NH_4H_2PO_4$ (+ B_2O_3)

S. Duan, Journal of Power Sources, Volume 449, 15 February 2020, 227574

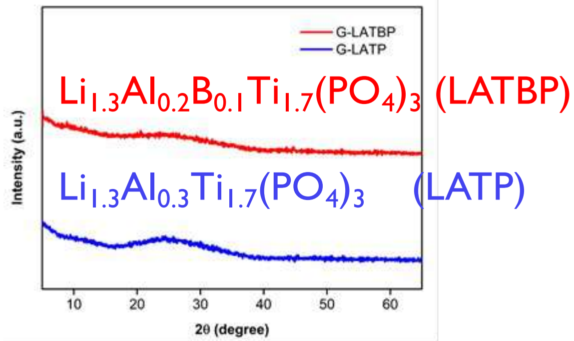

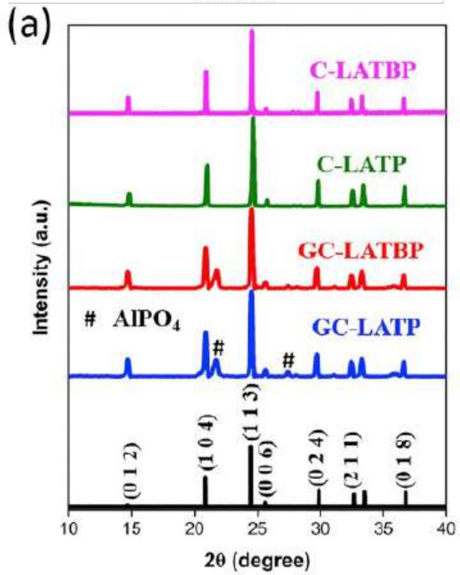

Ceramics (C-LATP and C-LATBP) conventional solid state method

Glass-Ceramics (GC-LATP and GC-LATBP)

$LiTi_2(PO_4)_3$

Stable crystalline phase with lower Grain-Boundary resistance

C-LATP GC-LATP GC-LATBP

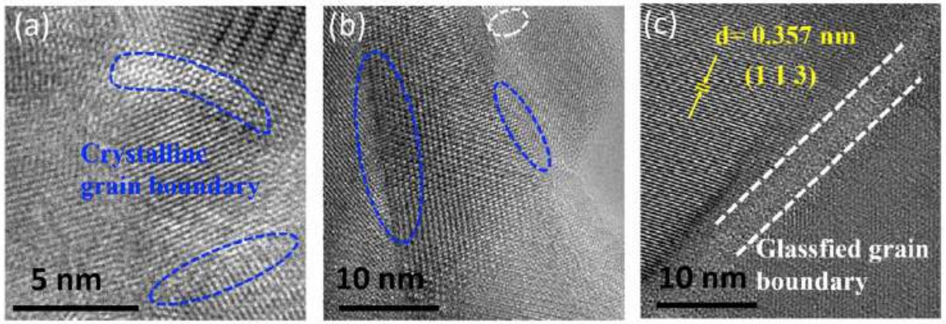

Amorphous phase at Grain Boundary

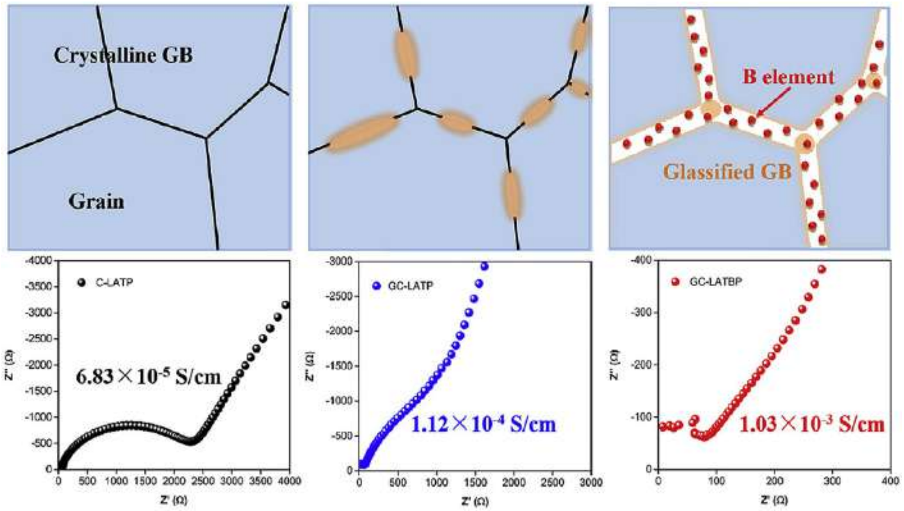

Arrhenius plots of bulk conductivity

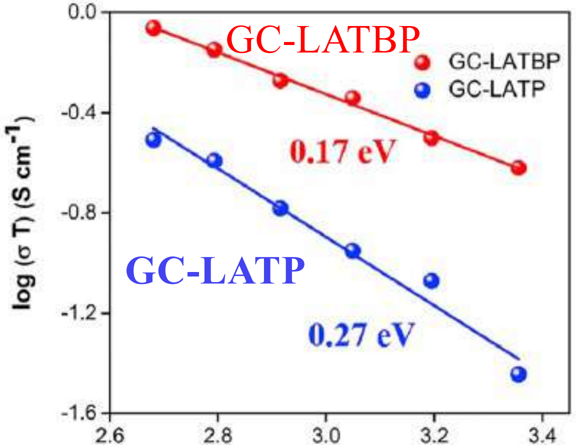

$$\sigma . T = A . exp\left(-\frac{E_a}{k_B . T}\right)$$

T Absolute temperature
k Boltzmann constant
A Pre-exponential factor

- grain boundary resistance of Ceramics, which also increases when boron is added
- inhomogeneous distribution of boron and glassified grain boundaries in Glass-Ceramics

⇒ reduces interfacial resistance at grain boundaries
⇒ higher conductivity in glass-ceramics, while boron can relax their grain boundaries even further.

S. Duan, Journal of Power Sources, Volume 449, 15 February 2020, 227574

Oxide Glass and Glass ceramic systems

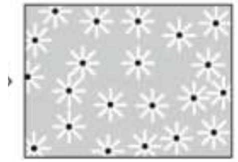

Review of various parameters of NASICON-type glass ceramic materials prepared by melt-quenching method

Composition	Tg (°C)	Tc (°C)	Crystallization	σ (S·cm^{-1})	E_a (eV)
$Li_{1.3}Al_{0.3}Ti_{1.7}(PO_4)_3$	624	660	1000 °C/0.33 h	1.3×10^{-3}	0.27
$Li_{1.3}Al_{0.3}Ti_{1.7}(PO_4)_3$	640	670	950 °C/70 h	1.23×10^{-4}	0.37
$Li_{1.3}Al_{0.3}Ti_{1.7}(PO_4)_3$-$50P_2O_5$	632	750	850 °C/10 h	8.5×10^{-4}	0.26
$Li_{1.4}Al_{0.4}Ge_{1.6}(PO_4)_3$	534	614	650 °C/96 h	3.8×10^{-5}	0.52
$Li_{1.5}Al_{0.5}Ge_{1.5}(PO_4)_3$	508.4	598.4	820 °C/2 h	5.03×10^{-4}	0.36
$Li_{1.5}Al_{0.5}Ge_{1.5}(PO_4)_3$	524	589	800 °C/8 h	2.9×10^{-3}	0.29
$Li_{1.25}Al_{0.25}Sn_{0.25}Ge_{1.75}(PO_4)_3$	518	622	628 °C/1 h	3.9×10^{-5}	0.36
$Li_{1.5}Al_{0.33}Sc_{0.17}Ge_{1.5}(PO_4)_3$			800 °C/8 h	5.8×10^{-3}	0.28
$Li_{1.5}Al_{0.5}Ge_{1.5}(PO_4)_3 + 0.05Li_2O$	532	629	829 °C/6 h	7.3×10^{-4}	0.38
$Li_{1.5}Al_{0.5}Ge_{1.5}(PO_4)_3$-$0.05B_2O_3$	526.0	636.4	820 °C/2 h	5.5×10^{-4}	
$Li_{1.4}Cr_{0.4}Ge_{0.64}Ti_{0.96}(PO_4)_3$	623	692	900 °C/12 h	6.6×10^{-5}	0.40
$Li_{1.6}Cr_{0.6}Ge_{0.28}Ti_{1.12}(PO_4)_3$	682.5	725.8	900 °C/2 h	2.9×10^{-4}	0.26

⇒ melt-quenching method still the mainstream preparation today

L. Lin, Materials **2023**, 16, 2655

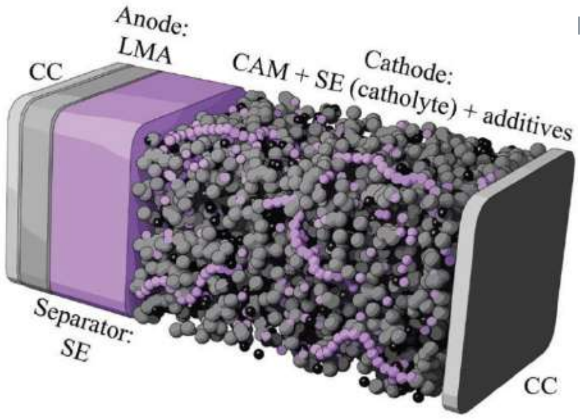

2 Glasses and glass-ceramics for Li-ion ASSB

2.1. Solid electrolytes (SE)

Oxides

Sulfides

2.2. All-Solid-State Batteries (ASSB)

From glass to glass-ceramic: $70Li_2S$-$30P_5S_5$

Mechanical milling
$Li_2S+P_2S_5$

Al_2O_3 balls and pot
20 h at 370 rpm

DTA curve for the $70Li_2S \cdot 30P_2S_5$ (mol %) mechanically milled sample.

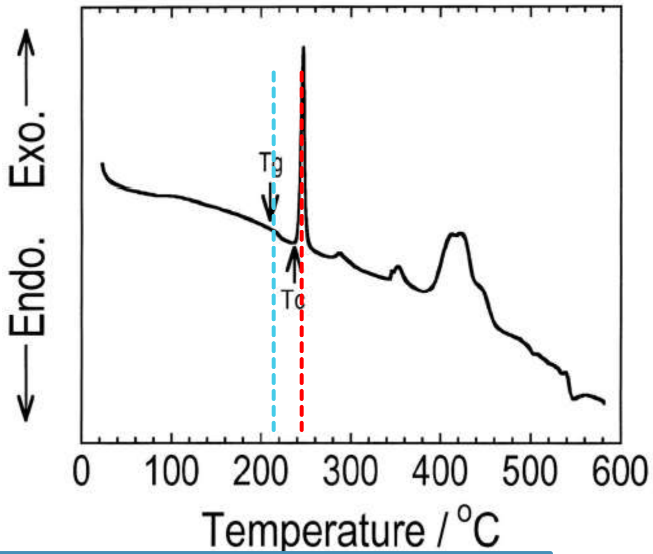

- Glass transition Tg is observed at around 210 °C
- Crystallization Tc is observed at 240 °C

Temperature dependences of the conductivities for $xLi_2S \cdot 100 - xP_2S_5$ mol % glass-ceramics with several compositions (Tc <T < 260°C)

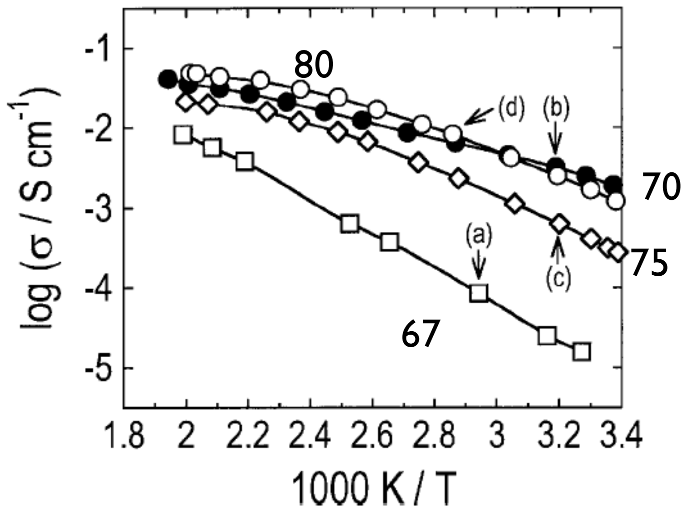

- $Li_4P_2S_6$ crystal with x = 67 mol, 10^{-6} $S.cm^{-1}$
- Highest conductivities with x = 70 and 80: glass-ceramic thio-LISICON II or III analog, 10^{-4} S cm^{-1}.

F. Mizuno, Electrochemical and Solid-State Letters, 8 (11) A603-A606 (2005)
New Lithium-Ion Conducting Crystal Obtained by Crystallization of the Li_2S–P_2S_5 Glasses

Glass-ceramic and superionic phase: $Li_7P_3S_{11}$

Mechanical milling
$Li_2S+P_2S_5$

Al_2O_3 balls and pot
20 h at 370 rpm

DTA curve for the $70Li_2S \cdot 30P_2S_5$ (mol %) mechanically milled sample.

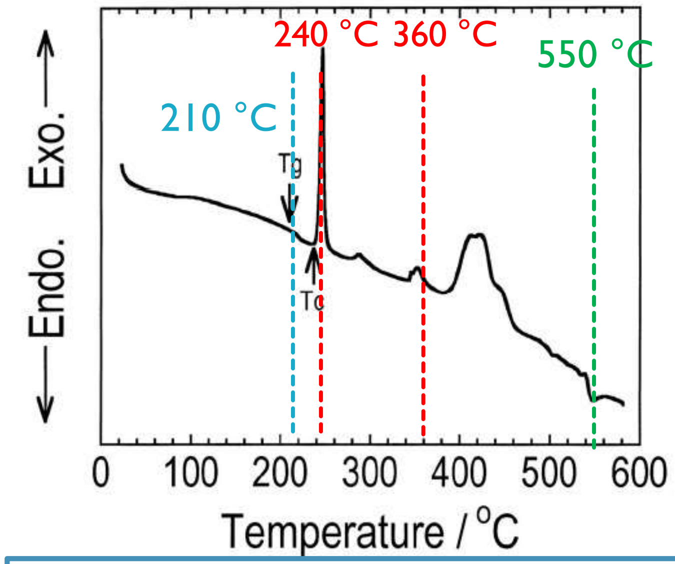

- Glass transition Tg is observed at around 210 °C
- Crystallization Tc is observed at 240 °C

XRD patterns of the $70Li_2S \cdot 30P_2S_5$ (mol %) glass-ceramics obtained by heating the glasses

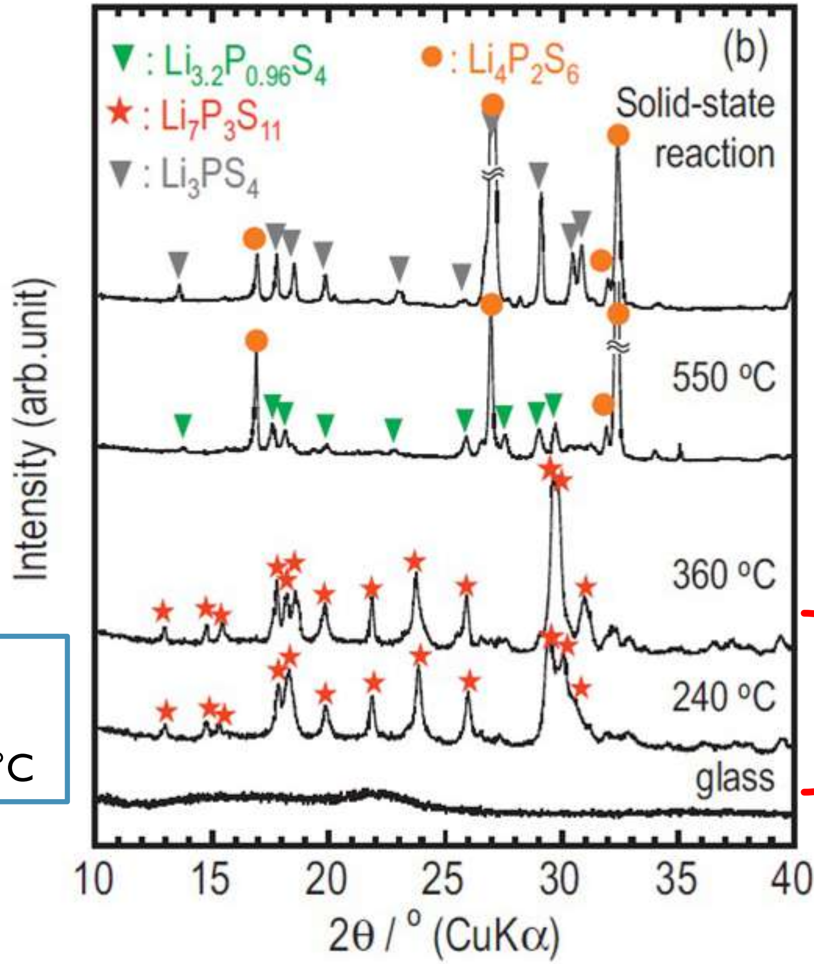

new crystalline phase

F. Mizuno, Electrochemical and Solid-State Letters, 8 (11) A603-A606 (2005)
New Lithium-Ion Conducting Crystal Obtained by Crystallization of the $Li_2S–P_2S_5$

Glass-ceramic and superionic phase: $Li_7P_3S_{11}$

$70Li_2S \cdot 30P_2S_5$ (mol%) glass

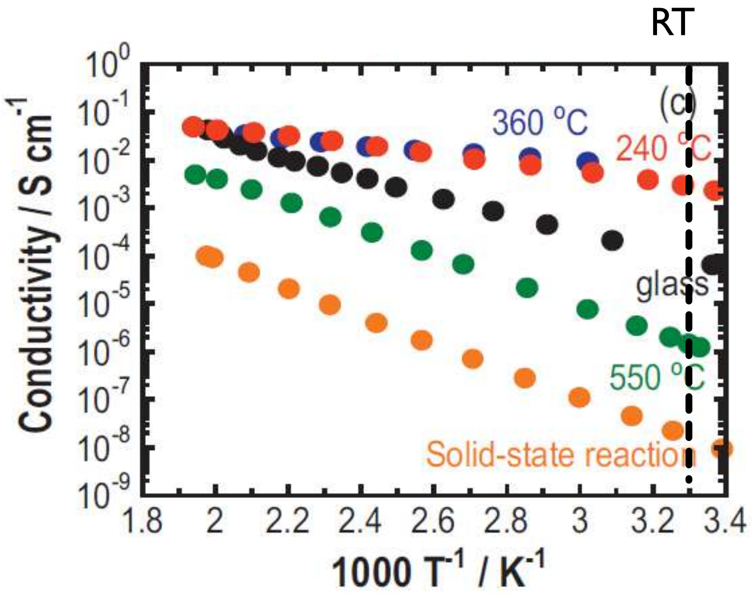

temperature dependence of conductivities
for the $70Li_2S \cdot 30P_2S_5$ (mol%) glass and glass–ceramics

highly conductive new crystalline phase

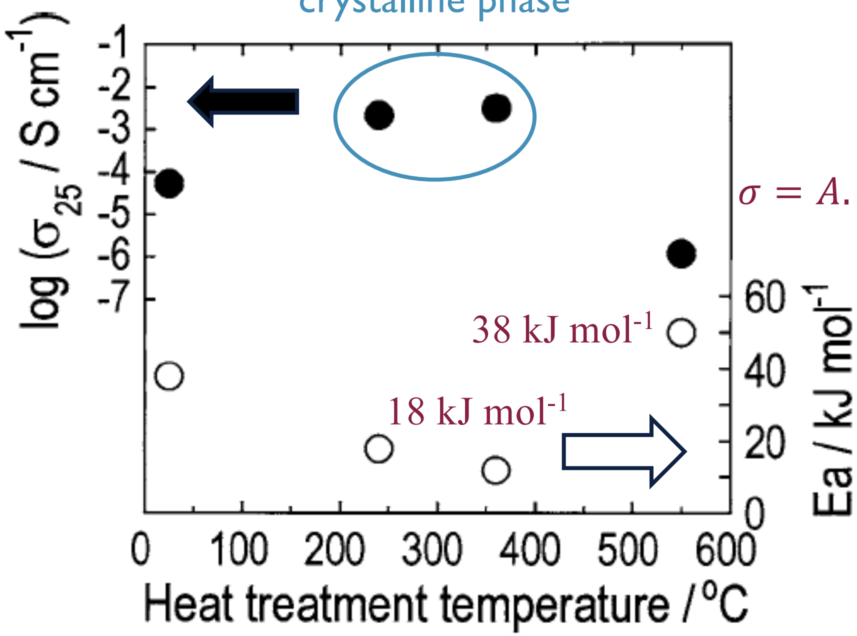

$$\sigma = A.exp\left(-\frac{E_a}{k.T}\right)$$

BM	glass	$\sigma_{ion(RT)} = 5.4 \times 10^{-5}$ S cm^{-1}
240 °C	glass-ceramic	$\sigma_{ion(RT)} = 2.2 \times 10^{-3}$ S cm^{-1}
360 °C	glass-ceramic	$\sigma_{ion(RT)} = 3.2 \times 10^{-3}$ S cm^{-1}
550 °C	Thio LISICON + $Li_4P_2S_6$	$\sigma_{ion(RT)} = 1.1 \times 10^{-6}$ S cm^{-1}
Solid state : Li_3PS_4 + $Li_4P_2S_6$		$\sigma_{ion(RT)} = 10^{-8}$ S cm^{-1}

F. Mizuno, Electrochemical and Solid-State Letters, 8 (11) A603-A606 (2005)

Glass-ceramic and superionic phase: $Li_7P_3S_{11}$

Structural model of superionic $Li_7P_3S_{11}$ crystal

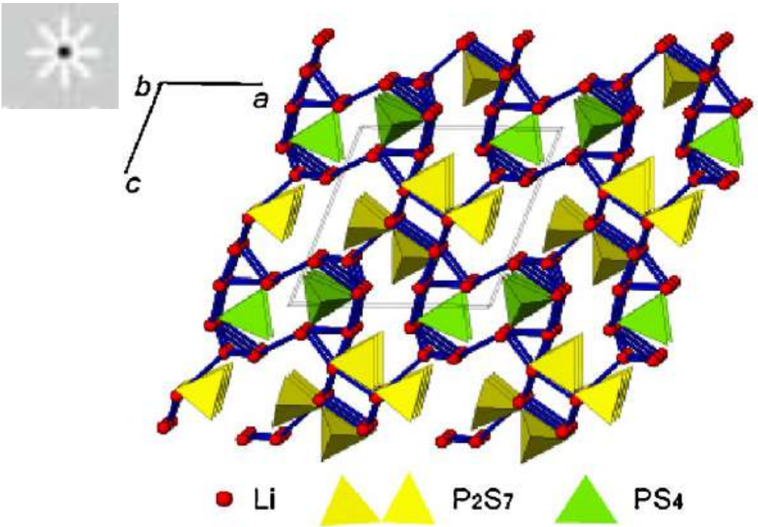

Li–Li correlations (solid blue lines) within 4 Å

- Triclinic cell (space group P−1)
- Both PS_4^{3-} tetrahedral and $P_2S_7^{4-}$ ditetrahedral ions are contained in the structure and Li^+ ions are situated between them.
- The crystal structure is completely different from other superionic conducting crystals such as $Li_{3.25}Ge_{0.25}P_{0.75}S_4$ and $Li_{10}GeP_2S_{12}$, which are composed of only tetrahedral ions (PS_4^{3-} and GeS_4^{3-}).
- Favorable Li^+ conduction path is presumably close to the Li–Li chains.

M. Tatsumisago, Journal of Asian Ceramic Societies 1 (2013) 17–25

synchrotron X-ray powder diffraction pattern.

Scalability of ball-milling process?
Compatibility with battery fabrication process?

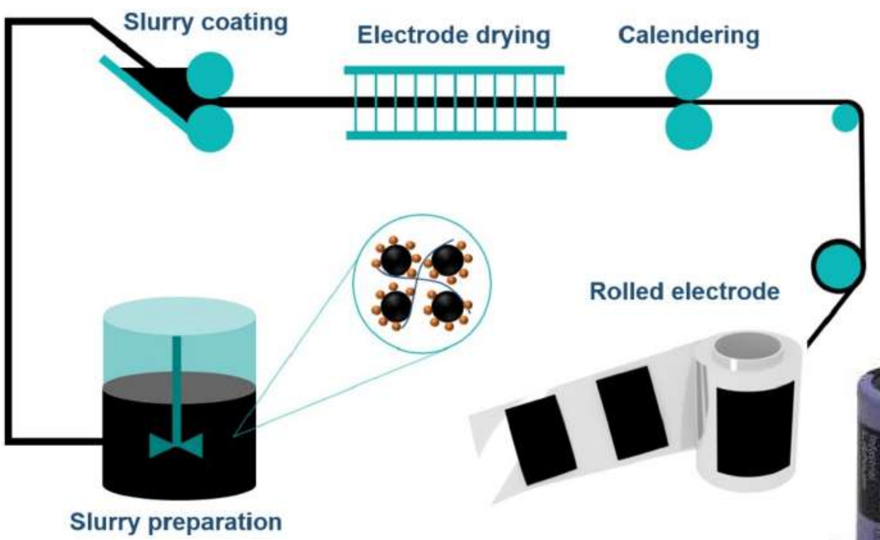

H. Liu, Particuology 57 (2021) 56–71

Assembling by wet-slurry process

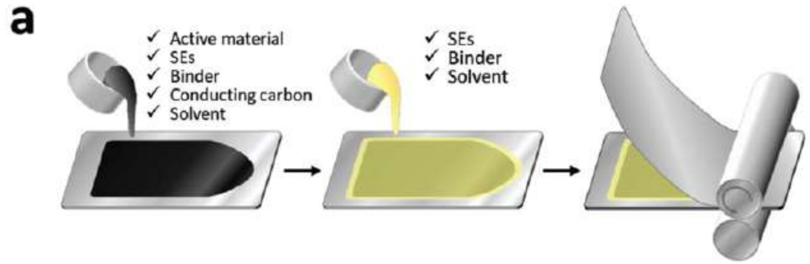

Application of solution-Processable SE for ASSB: impregnation

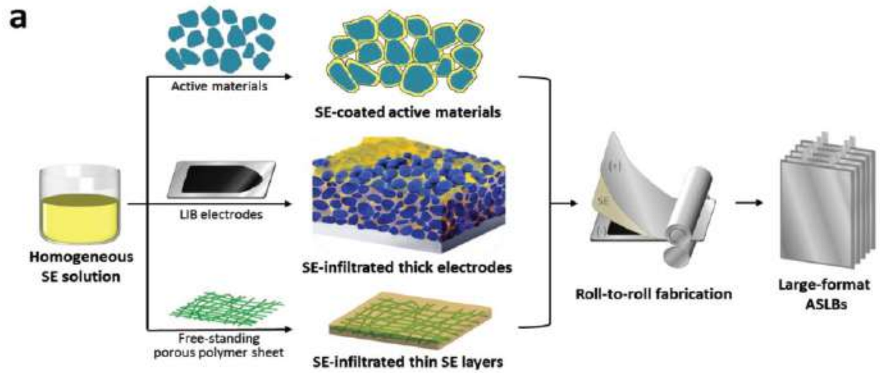

K. H. Park *et al.*, Adv. Energy Mater. 2018, 8, 1800035

Solvent assisted synthesis

Solvent Assisted Synthesis of GC-$Li_7P_3S_{11}$

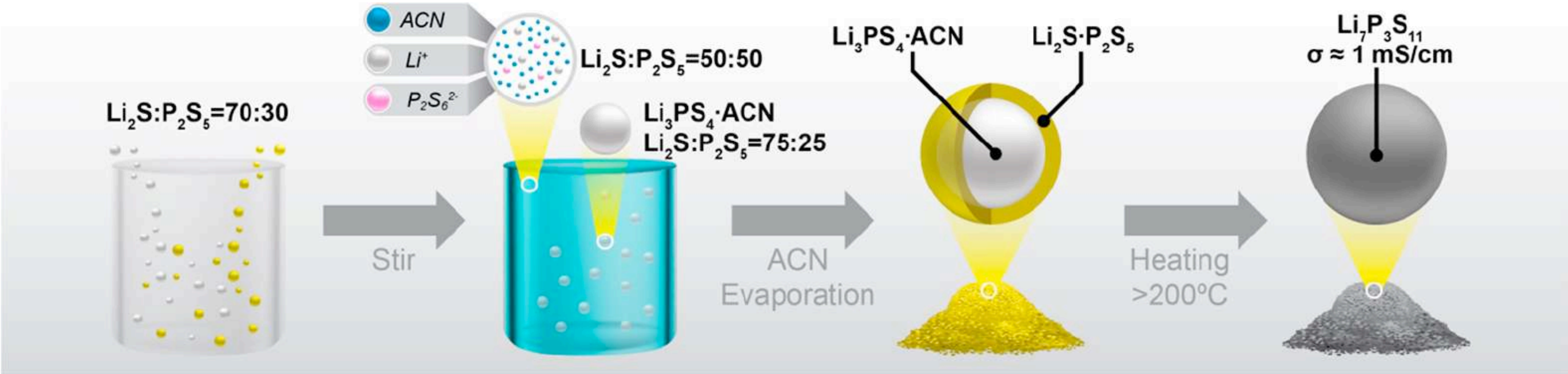

- Mixture of Li_3PS_4 and 50:50 Li_2S-P_2S_5 powder obtained after drying ACN
- Formation of GC-$Li_7P_3S_{11}$ after heating
- Formation of GC-$Li_7P_3S_{11}$ requires T > 260 °C

Wang et al., Chem. Mater. 30 (3), 990, 2018

Solvent Assisted Synthesis of GC-$Li_7P_3S_{11}$

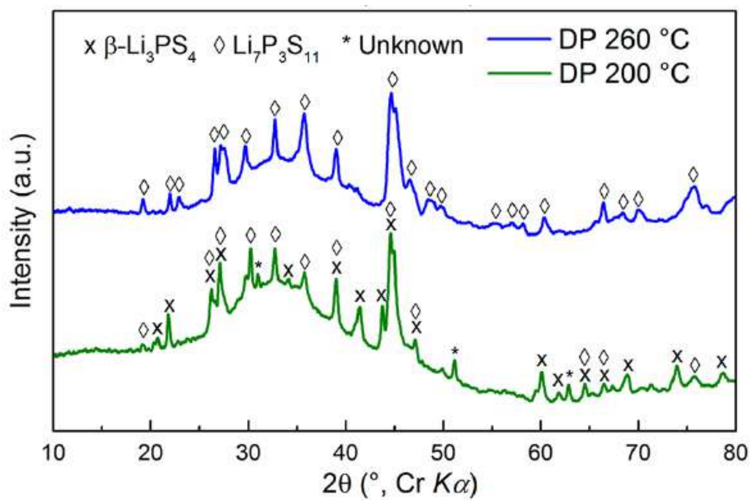

Raman

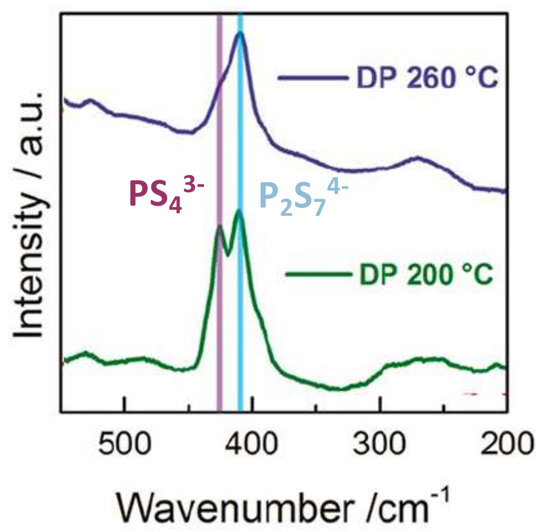

^{31}P MAS NMR

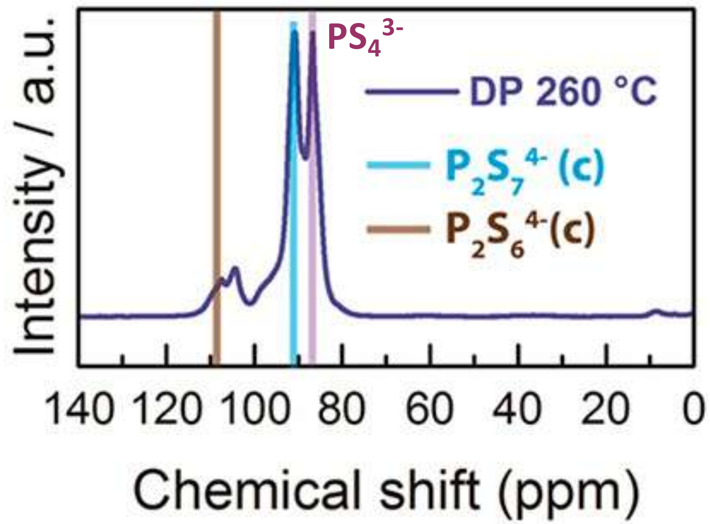

Metastable crystal mainly composed of the $P_2S_7^{4-}$ (pyrothiophosphate) ions
thio-LISICONs Li_3PS_4 consisting of PS_4^{3-} (ortho-thiophosphate) ions
structural unit of $P_2S_6^{4-}$ in the crystalline $Li_4P_2S_6$ phase

- Below 260 °C, crystallization of β-Li_3PS_4
- T > 260 °C required for complete stoichiometric reaction and $Li_7P_3S_{11}$ formation

Wang et al., Chem. Mater. 30 (3), 990, 2018

Improvement of the stability of sulfide electrolytes

- substitution engineering of O to S
- replacement of P and S elements with congeners, such as more polarizable Sb and more stable O (theory of hard and soft acid−base (HSAB))

Li_3PS_4

↓ Sn, Sb, Zn

$Gc\text{-}Li_{3.2}P_{0.8}Sn_{0.2}S_4$

B.H. Zhao, Adv. Mater. 2021, 33, 2006577

$Li_7P_3S_{11}$

↓ Sb ↓ O

$Li_7P_{2.9}Sb_{0.1}S_{10.75}O_{0.25}$

B.H. Zhao, ACS Appl. Mater. Interfaces 2021, 13, 34477−34485

Goal
- To increase the air-stability
- To improve the Li metal compatibility

Improvement of the stability of sulfide electrolytes

$Li_7P_3S_{11}$

Sb ↓ ↓ O

$Li_7P_{2.9}Sb_{0.1}S_{10.75}O_{0.25}$

- substitution engineering of O to S
- replacement of P and S elements with congeners, such as more polarizable Sb and more stable O (theory of hard and soft acid–base (HSAB))

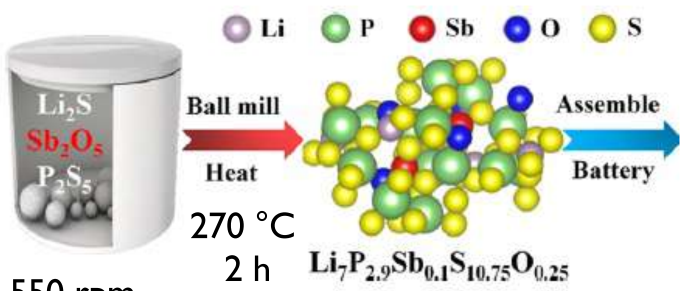

550 rpm
30 h
RT

270 °C
2 h

$Li_7P_{3-x}Sb_xS_{11-2.5x}O_{2.5x}$
(x = 0, 0.04, 0.08, 0.1, 0.12, and 0.16)

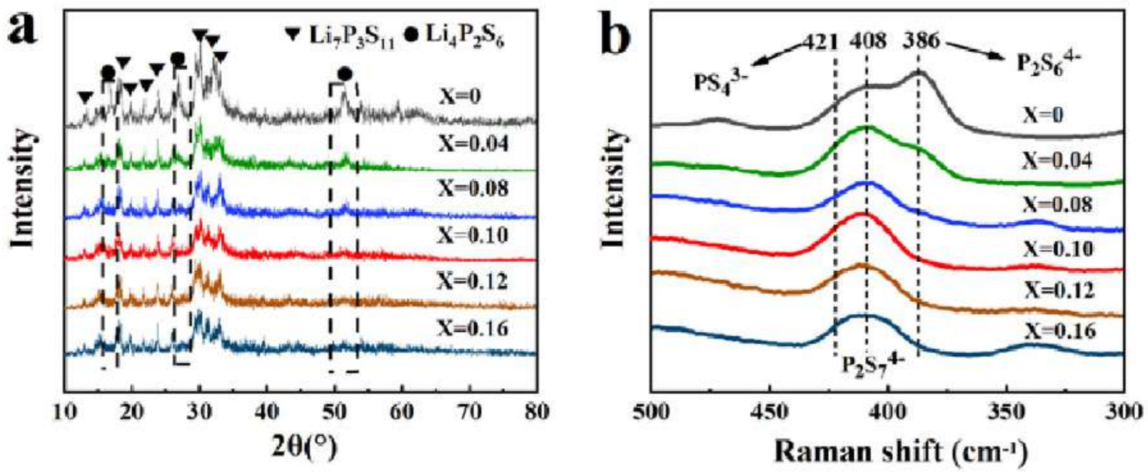

x = 0
x = 0.04
x = 0.08
x = 0.1
x = 0.12
x = 0.16

- Pure $Li_7P_3S_{11}$ for x ≥ 0,10
- no diffraction peaks of Sb_2O_5

⇒ Sb and O successfully incorporated

B.H. Zhao, ACS Appl. Mater. Interfaces 2021, 13, 34477–34485
Congener Substitution Reinforced $Li_7P_{2.9}Sb_{0.1}S_{10.75}O_{0.25}$ Glass-Ceramic Electrolytes for All-Solid-State Lithium–Sulfur Batteries

Improvement of the stability of sulfide electrolytes

Nyquist plots
SS/solid-state electrolyte/SS cells

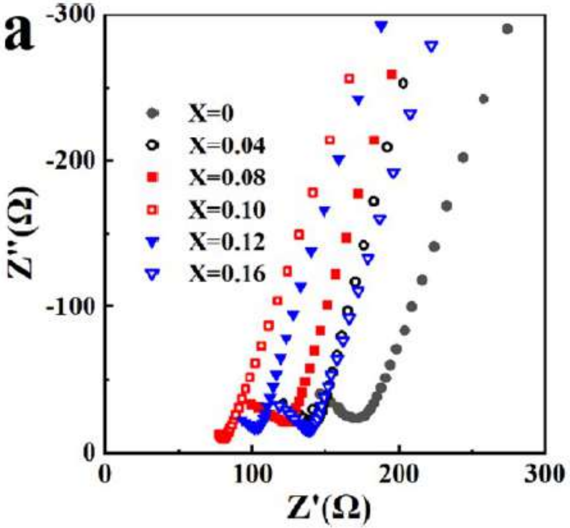

Arrhenius plots of ionic conductivity

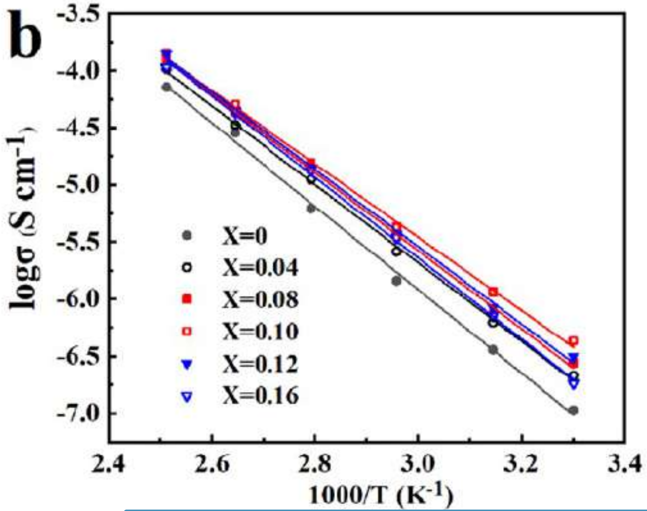

- σ ↑ from x=0 to x=0.1 then ↓
- σ_{ion} for 0=0.10 is 2.2 times higher than that of the pristine $Li_7P_3S_{11}$

- Smallest activation energy E_a of x = 0.10,
- The pristine $Li_7P_3S_{11}$ electrolyte presents the largest E_a value

$Li_7P_3S_{11}$

Sb ↓ ↓ O

$Li_7P_{2.9}Sb_{0.1}S_{10.75}O_{0.25}$

$Li_7P_{3-x}Sb_xS_{11-2.5x}O_{2.5x}$
(x = 0, 0.04, 0.08, 0.1, 0.12, and 0.16)

$$\sigma = A.\exp\left(-\frac{E_a}{k.T}\right)$$

X	conductivity (σ, S cm^{-1})	Ea (kJ mol^{-1})
0	7.26×10^{-4}	30.3
0.04	9.06×10^{-4}	28.5
0.08	1.04×10^{-3}	28.4
0.10	1.61×10^{-3}	26.6
0.12	1.22×10^{-3}	28.1
0.16	8.98×10^{-4}	29.3

B.H. Zhao, ACS Appl. Mater. Interfaces 2021, 13, 34477−34485

Improvement of the stability of sulfide electrolytes

$Li_7P_3S_{11}$

Sb ↓ ↓ O

$Li_7P_{2.9}Sb_{0.1}S_{10.75}O_{0.25}$

Quantity of H_2S gas during air exposure

amount of H_2S gas generated after 4000 s air exposure tests.

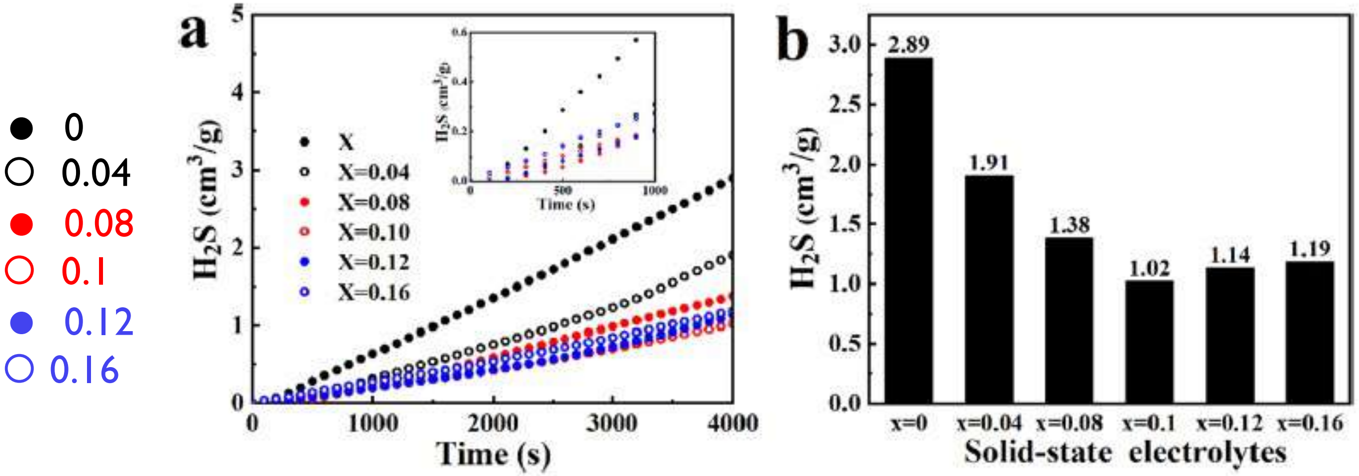

$Li_7P_{3-x}Sb_xS_{11-2.5x}O_{2.5x}$
(x = 0, 0.04, 0.08, 0.1, 0.12, and 0.16)

- Water in humid air can hydrolyze sulfide electrolyte and produce harmful H_2S, ultimately decomposing the electrolyte and reducing ionic conductivity.
- Amount of H_2S gas generated is gradually increased during the exposure.
- Pristine $Li_7P_3S_{11}$ electrolyte shows the fastest growing speed among all of the samples.

B.H. Zhao, ACS Appl. Mater. Interfaces 2021, 13, 34477−34485
Congener Substitution Reinforced $Li_7P_{2.9}Sb_{0.1}S_{10.75}O_{0.25}$ Glass-Ceramic Electrolytes for All-Solid-State Lithium−Sulfur Batteries

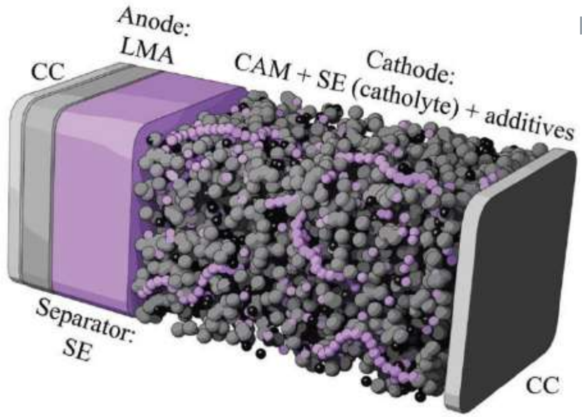

2 Glasses and glass-ceramics for Li-ion ASSB

2.1. Solid electrolytes (SE)

Oxides

Sulfides

2.2. All-Solid-State Batteries (ASSB)

Principle of a conventional lithium-ion battery

$C_{graphite}$ $LiCoO_2$

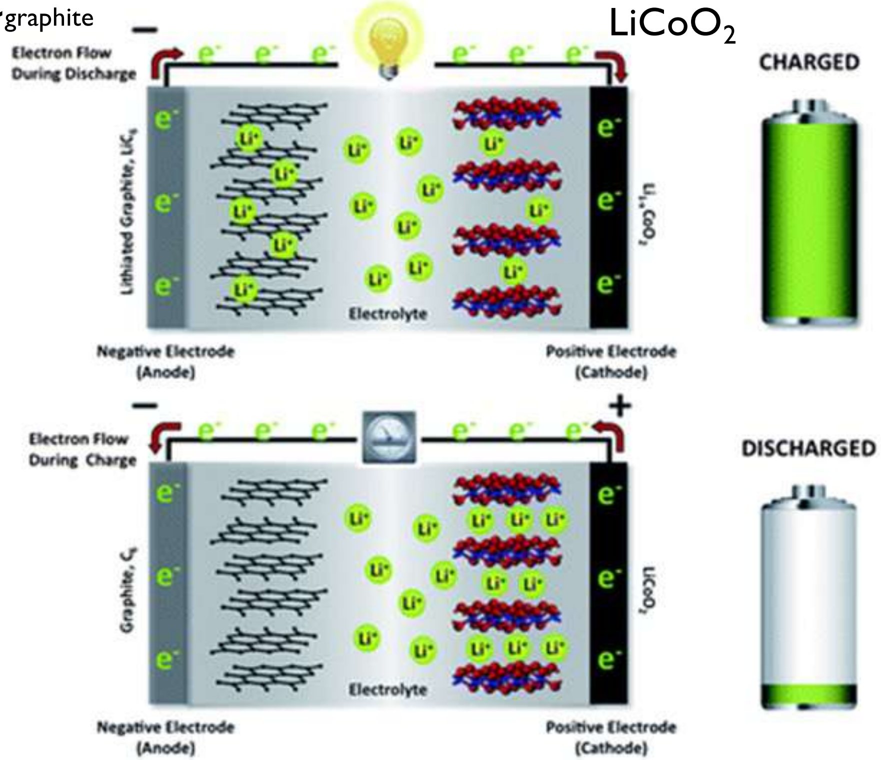

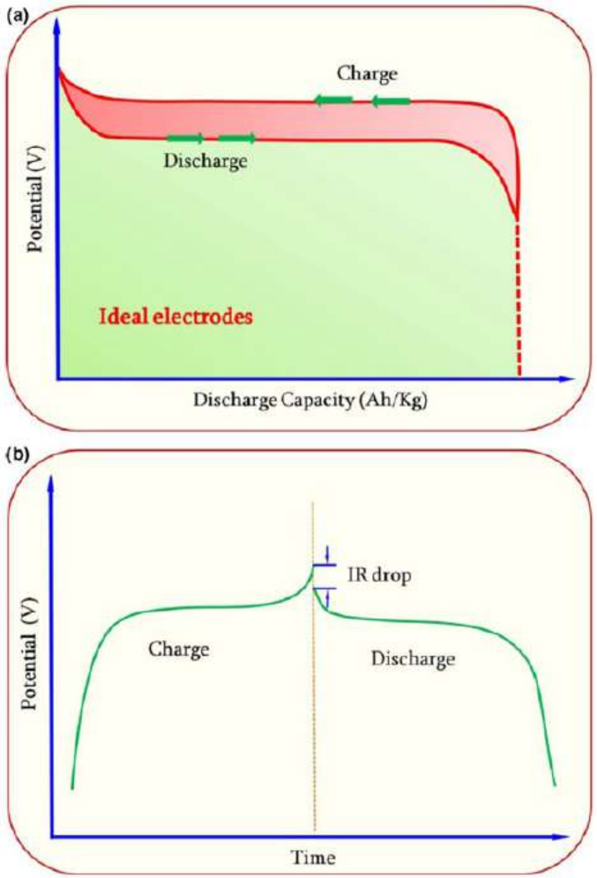

Capacity C (A.h)

$$C = \frac{F.x}{3600.M} = \frac{96485.x}{3600.M}$$

$C_{cathode}(LiCoO_2)_{theo}$ = 135 mAh.g^{-1}

$C_{anode}(C_6)_{theo} = \frac{96485.1}{3600.(6\times12)} =$
= 372 mAh.g^{-1}

Charge of the battery

$LiCoO_2 \Leftrightarrow Li_{1-x}CoO_2 + x\,Li^+ + x\,e^-$ (x_{max} =0,5)

$6C + x\,Li^+ + x\,e^- \Leftrightarrow Li_xC_6$

Energy

$E = \frac{C_c \times C_a}{C_c + C_a} \times V_{cell}$

Power

$P = V_{cell} \times I$

Challenges for the ASSB assembling

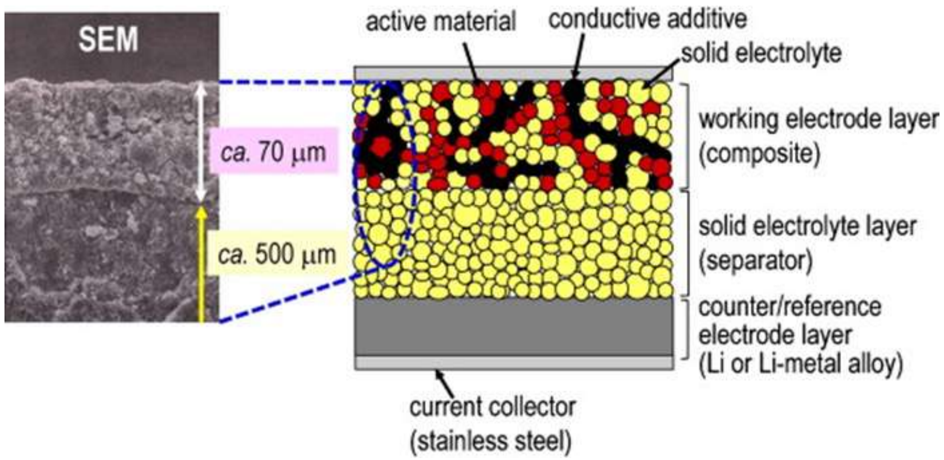

M. Tatsumisago, Journal of Asian Ceramic Societies 1 (2013) 17–25.

Importance of:

- Conductive additives
- Active material
- Binders
- Formulation (ratios of ≠ components)
- Mixing method (hand grinding, turbula,..)

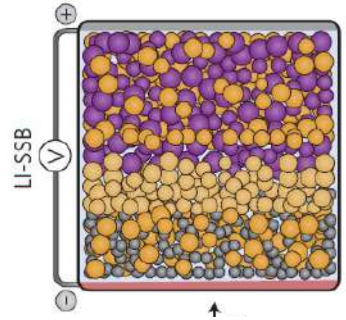

Cathode composite

Solid electrolyte

Anode composite

SEM pictures

$LiCoO_2$ electrolyte $80Li_2S$-$20P_2S_5$

different conductive additives:

acetylene black VGCF

TiN Ni

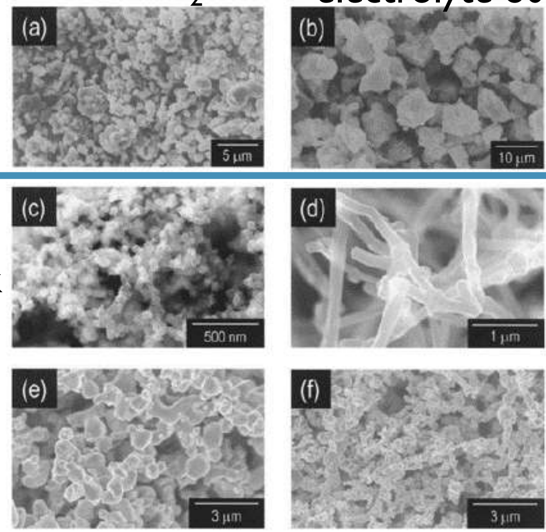

F. Mizuno, Journal of the Electrochemical Society 152(8) (2005) A1499

Assembling processes

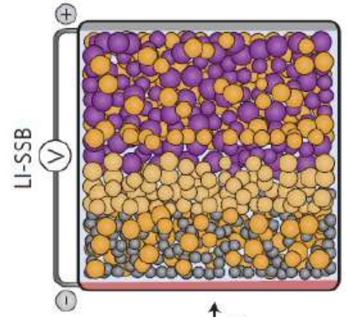

Cathode composite

Solid electrolyte

Anode composite

powder pressing process (lab scale)

e

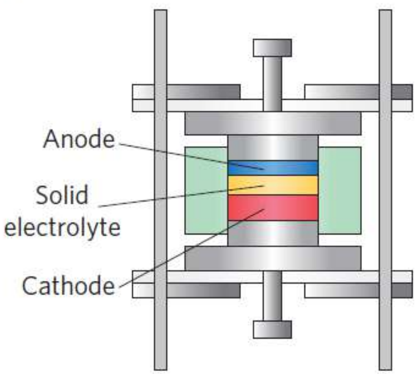

- Sulfides are ductile
- easily form dense cathode and anode composites

far fewer examples of all-solid batteries with oxides than with sulfides

difficult to scale up for practical applications

Some alternative fabrication methods may be considered

Solution processed (industrial scale)

g

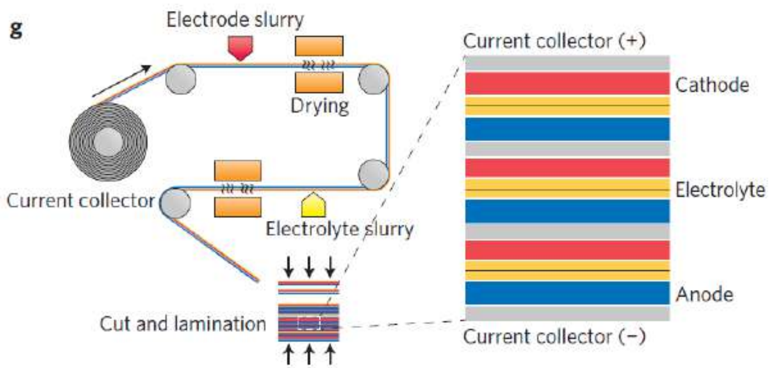

Investigation of solvents of polymer binders

Yong-Sheng Hu, Nature Energy, Vol. 1, 2016, article number: 16042

Li ion batteries: large choice of active materials

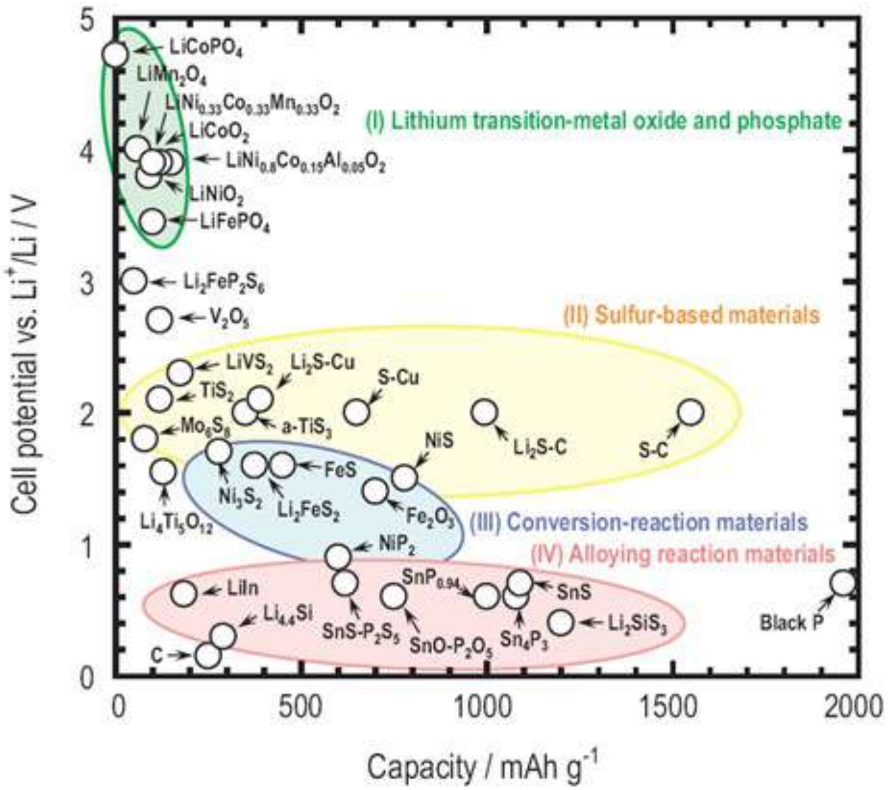

Four categories on the basis of cell potential:

(I) lithium transition-metal oxides and phosphates with a potential of 3.5–5 V (●), category including high-potential positive electrodes:

- $LiCoO_2$,
- $LiNiO_2$,
- $LiNi_{0.8}Co_{0.15}Al_{0.05}O_2$,
- $LiNi_{0.33}Co_{0.33}Mn_{0.33}O_2$,
- $LiMn_2O_4$,
- $LiFePO_4$
- and $LiCoPO_4$.

(II) sulfur-based materials with 2 V (●),

(III) conversion-reaction materials with 1–2 V (●),

(IV) alloying reaction materials with below 1 V (●).

M. Tatsumisago, Journal of Asian Ceramic Societies 1 (2013) 17–25.

Charge–discharge curves at the 500th cycle of In/$LiCoO_2$ cells with the $80Li_2S \cdot 20P_2S_5$ glass-ceramic

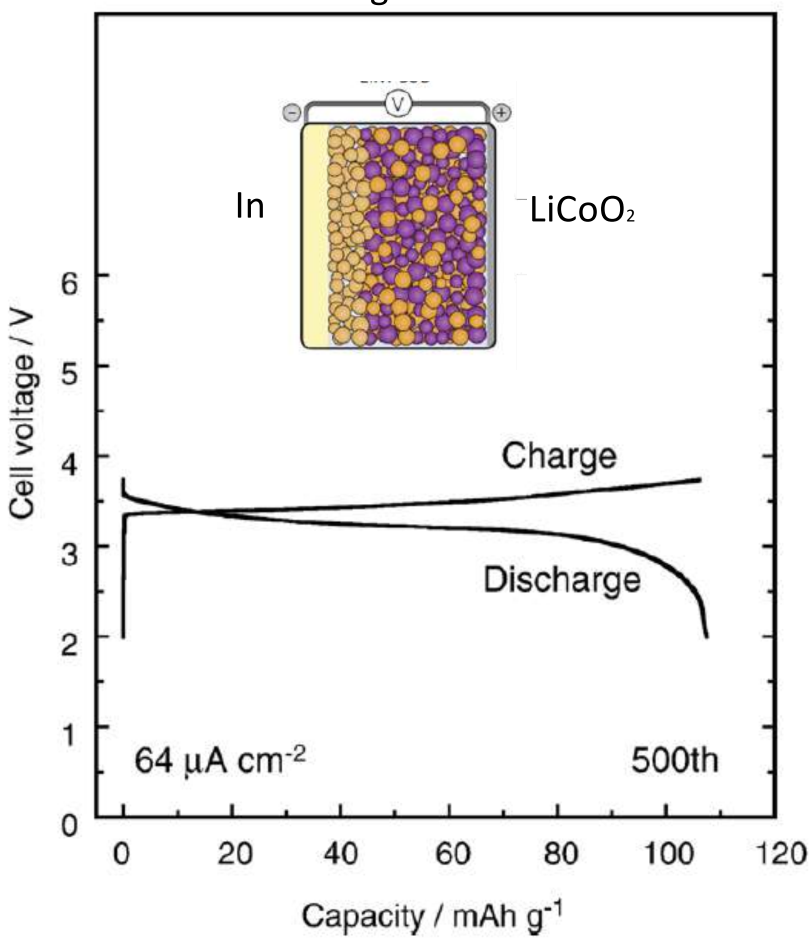

Li-ion batteries

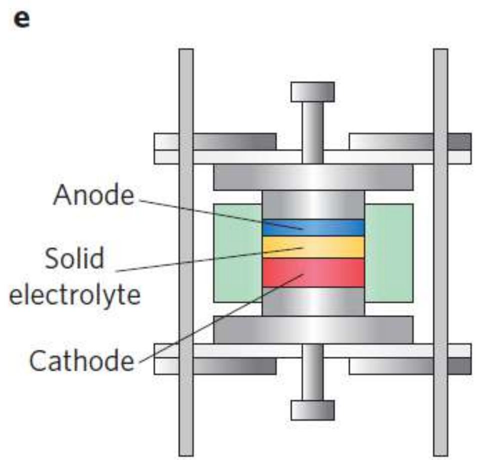

negative electrode
indium foil with a thickness of 0.1 mm
pressed under 2.5×10^8 Pa on the pellet

80 mg glass-ceramics powder
acting as a solid electrolyte

20 mg composite cathode
$LiCoO_2$, glass-ceramics and acetylene-black with the weight ratio of 20:30:3.

⇒ obtained In/$LiCoO_2$ cells charged and discharged at room temperature in an Ar atmosphere (glove-box).

- Irreversible capacity initially observed at the first few cycles,
- The all-solid-state cell maintains the reversible capacity of about 100 mA.h g^{-1}

Recent progress of glass and glass-ceramics as solid electrolytes for lithium secondary batteries.
T. Minami et al., Solid State Ionics 2006, 177, 2715–2720.

Charge–discharge curves at the 500th cycle of In/$LiCoO_2$ cells with the $80Li_2S{\cdot}20P_2S_5$ glass-ceramic

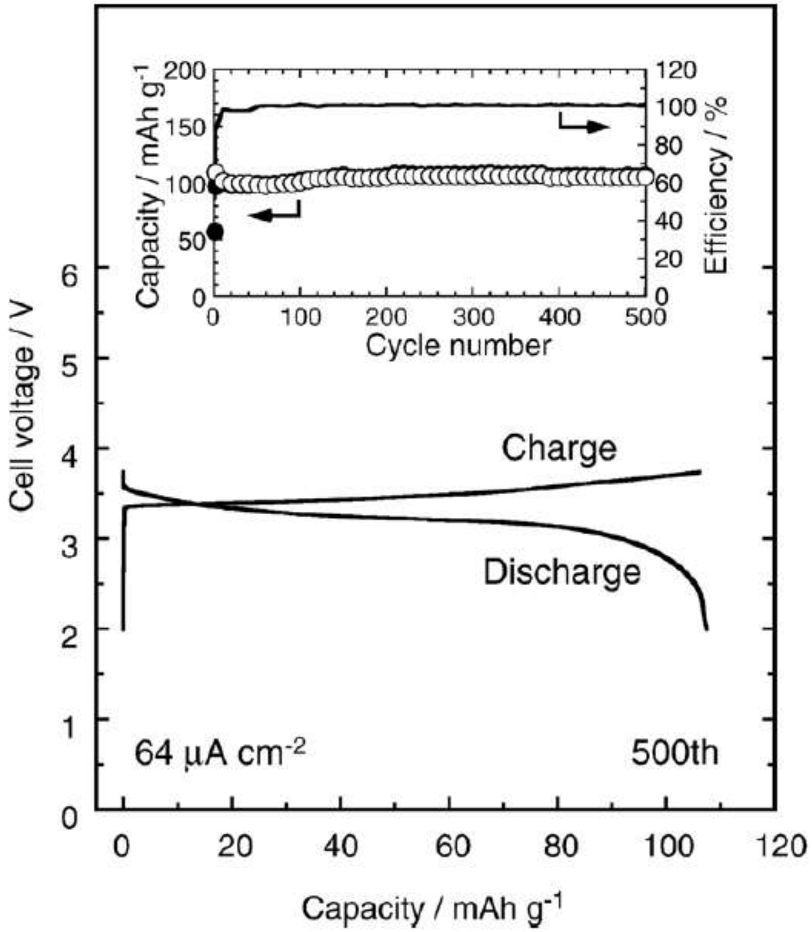

Li-ion batteries

Battery's performance evaluated based on:

Retention of capacity over iterative cycling: Coulombic efficiency (CE)
= percent of specific discharge (A.h/kg or A.h/l) retained upon immediate subsequent charging.
CE is always less than 100% for real SIBs

(Lifetime of a SIB often defined as the number of cycles until the cell only demonstrates 80% of its initial capacity, so a cell which has a lifetime of 500 cycles must have a CE of at least 99.96% for each cycle)

Charge–discharge efficiency of 100% (no irreversible capacity) for 500 cycles,
⇒ the cell works as a lithium secondary battery without the decomposition of the glassy electrolyte.

Recent progress of glass and glass-ceramics as solid electrolytes for lithium secondary batteries.
T. Minami et al., Solid State Ionics 2006, 177, 2715–2720.

Charge–discharge cycle performance
of the all-solid-state Li–In/$Li_4Ti_5O_{12}$ cell

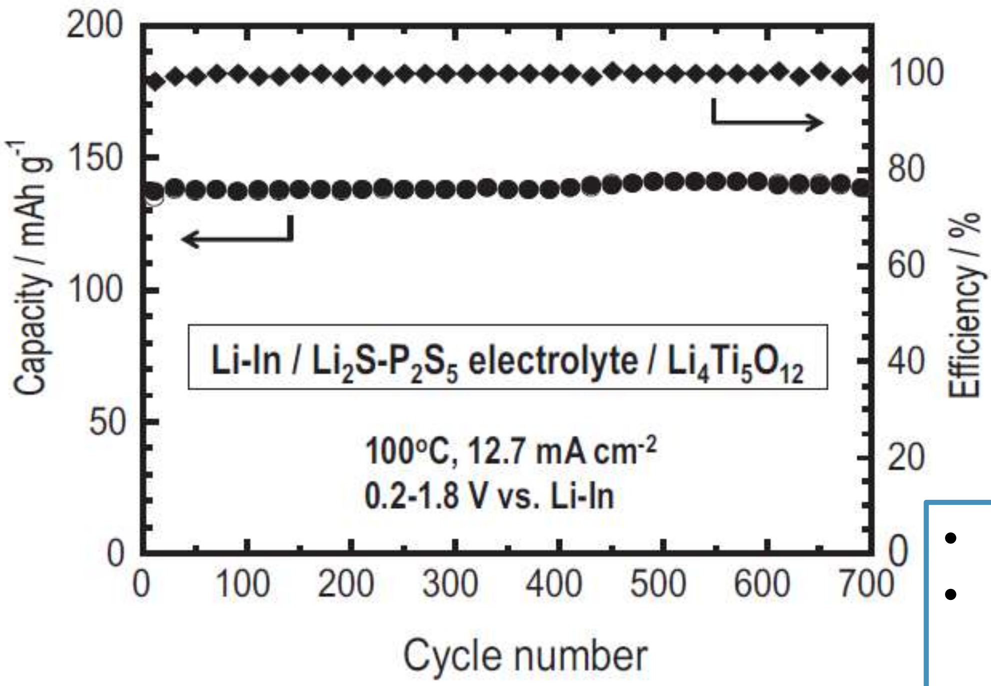

M. Tatsumisago, M. Nagao, A. Hayashi,
Journal of Asian Ceramic Societies 1 (2013) 17–25.

Li-ion batteries

$Li_4Ti_5O_{12}$
Commercialized negative electrode
Moderate potential of 1.55 V (vs. Li^+/Li) but "zero-strain" material during charge–discharge processes

Composite working electrode
= $Li_4Ti_5O_{12}$, Li_2S–P_2S_5 glass–ceramic SE, and vapor grown carbon fiber (VGCF) powders with a weight ratio of 38:58:4

Cycling at 100 °C!

- Discharge and charge capacity of about 140 $mAhg^{-1}$
- Capacity maintained for 700 cycles with no degradation under a high current density of over 10 mA cm^{-2}.

⇒ all-solid-state batteries using glass–ceramic electrolytes have a benefit of high temperature application.

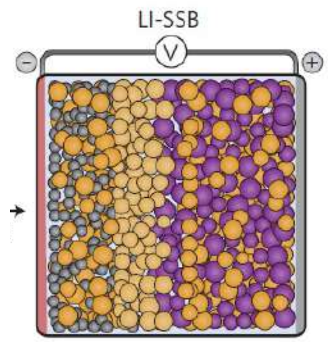

3

Na-based All-Solid-State Batteries

Cathode active materials and solid electrolytes

From Lithium to sodium

Lithium demand by end use

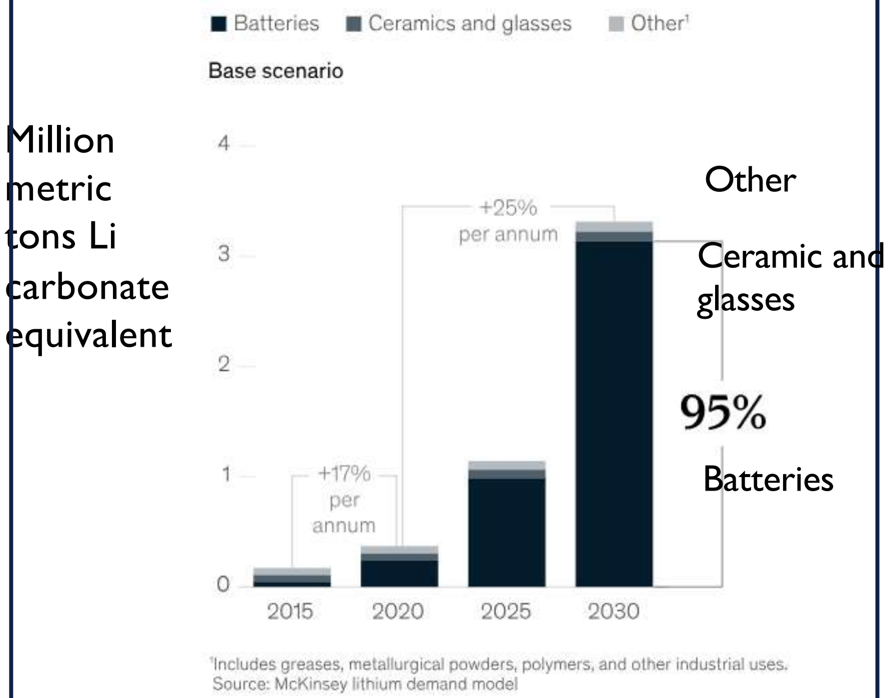

By 2030, batteries are expected to account for 95 percent of lithium demand, and total needs will grow annually by 25 to 26 percent to reach 3.3 million to 3.8 million metric tons LCE

Global lithium supply and demand

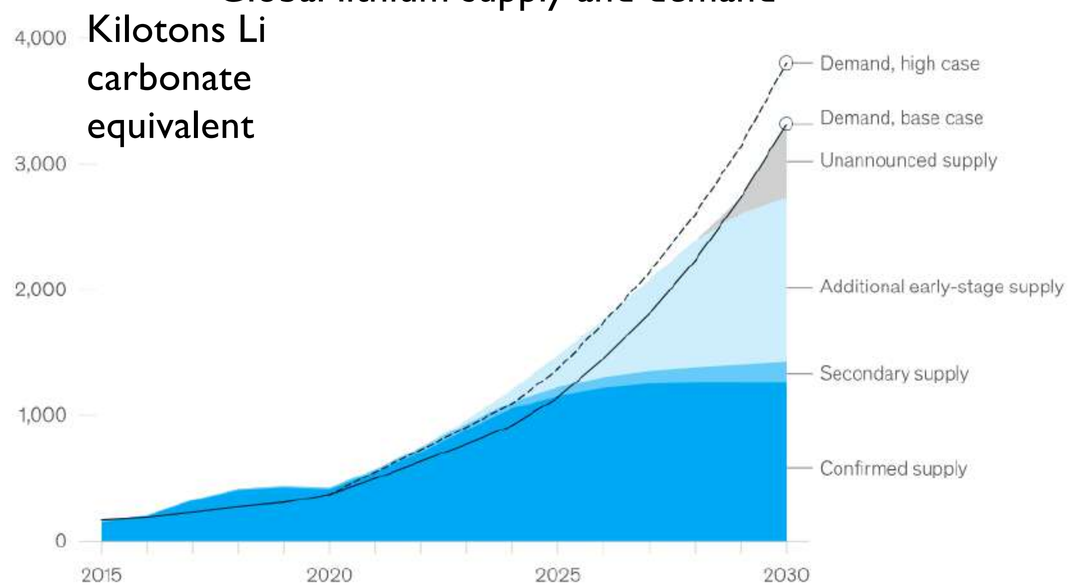

Possible shortage by 2025!

- forecasted demand and supply indicates a balanced industry for the short term
- potential need to galvanize new capacity by 2030:
  Additional lithium sources required to bridge the supply gap
- new technologies such as DLE and DLP are expected to boost recovery and capacity.

McKinsey: Lithium Mining, How new production technologies could fuel the global EV revolution (April 2022)

From Lithium to sodium

Element abundance in Earth's crust

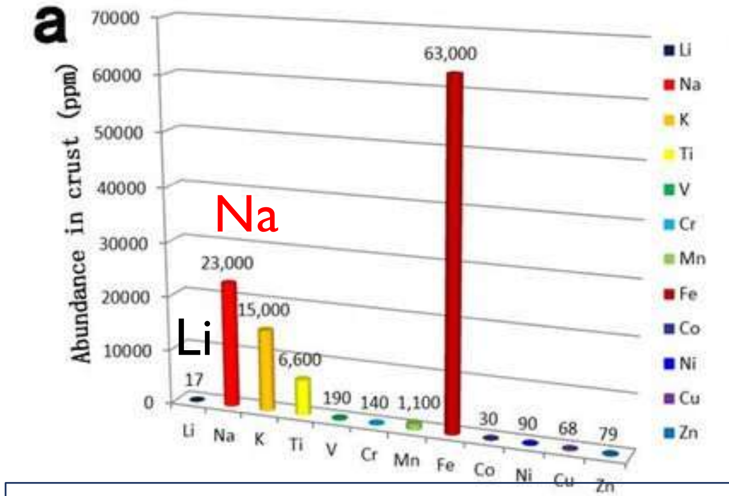

The world distribution of lithium resource

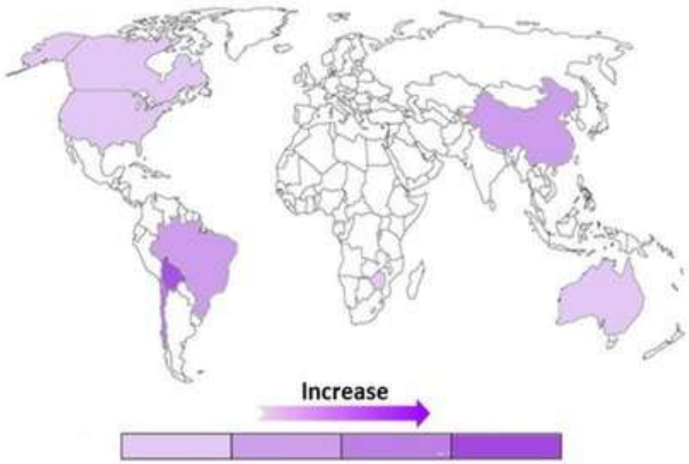

large-scale applications of LIBs in portable electronics and electric vehicles (EV) market + application of LIBs in stationary energy storage

⇒ uneconomical in the near future.

⇒ increase of price of Li resources due:

- to its low abundance in the Earth’s crust
- and its non-uniform geographic distribution

development of low-cost, highly-safe and cycling stable rechargeable batteries based on abundant resources is becoming urgent and highly desired.

⇒ Na

Y. Li, et al., *Energy Storage Materials* 7 (2017): 130-151.

From Lithium to sodium with liquid based batteries

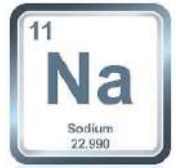

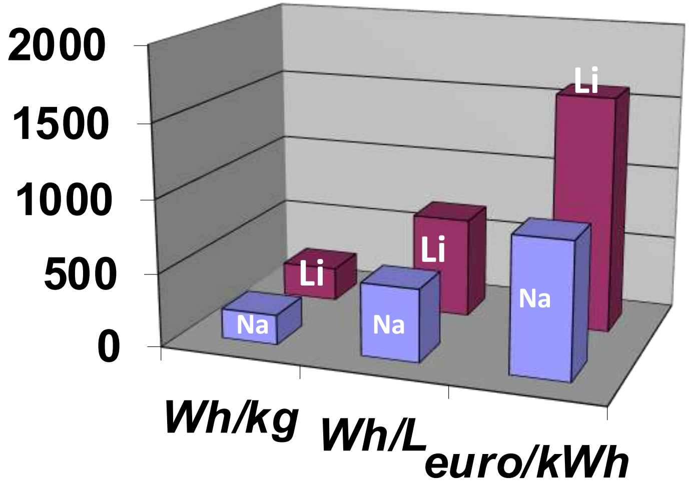

Sodium-ion batteries (SIBs):

- large energy density of ~150 Wh kg^{-1},

⇒ currently attracting the attention of both academic and industrial research communities due to their potential for meeting the growing needs of the grid and transportation sectors

Sodium-ion battery technology was discovered in the early 1970 and 80s, but it is less popular compared to current lithium-ion battery technology due to poor energy density and low cycle stability of SIBs, which hinders their practical application.

SIBs are the best alternative choice to LIBs because of:

(i) SIBs and LIBs sharing the similar operating principle,
(ii) cheaper and abundant raw materials,
(iii) water-based electrolytes
(iv) replace the cupper collectors with aluminum collectors, and
(v) stable electrochemical potential window (-2.71 V vs. SHE)

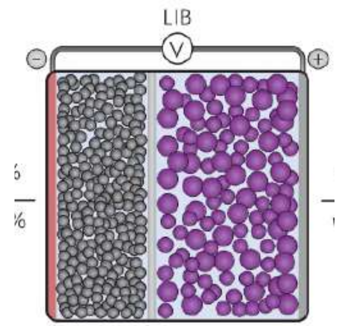

From Lithium to sodium with liquid based batteries

Na-ion

towards marketing…

2017 creation of TIAMAT start-up,
hosted in the HUB of Energy (Amiens), 15 people

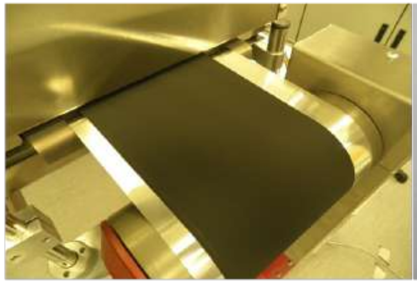

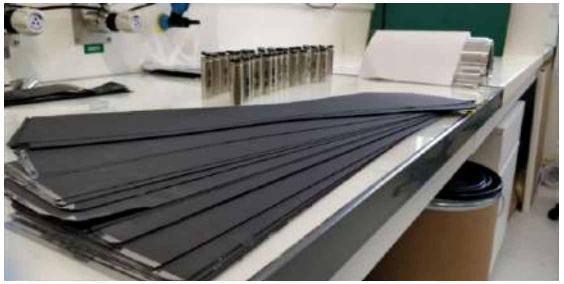

http://www.tiamat-energy.com/

100 cells / month
In September 2018

↓

200 cells / month
in October 2018

↓

500 cells / month

JUST RELEASED
(October 2023)

need for
power and
fast recharging

High Power density
2-5 kW/kg

Long Lifetime
5000+ cycles
up to 80% of capacity

High level of safety

construction of the Mega factory near Amiens by 2025

Na batteries

The relationship between capacity and voltage for present electrode materials in Na-ion batteries

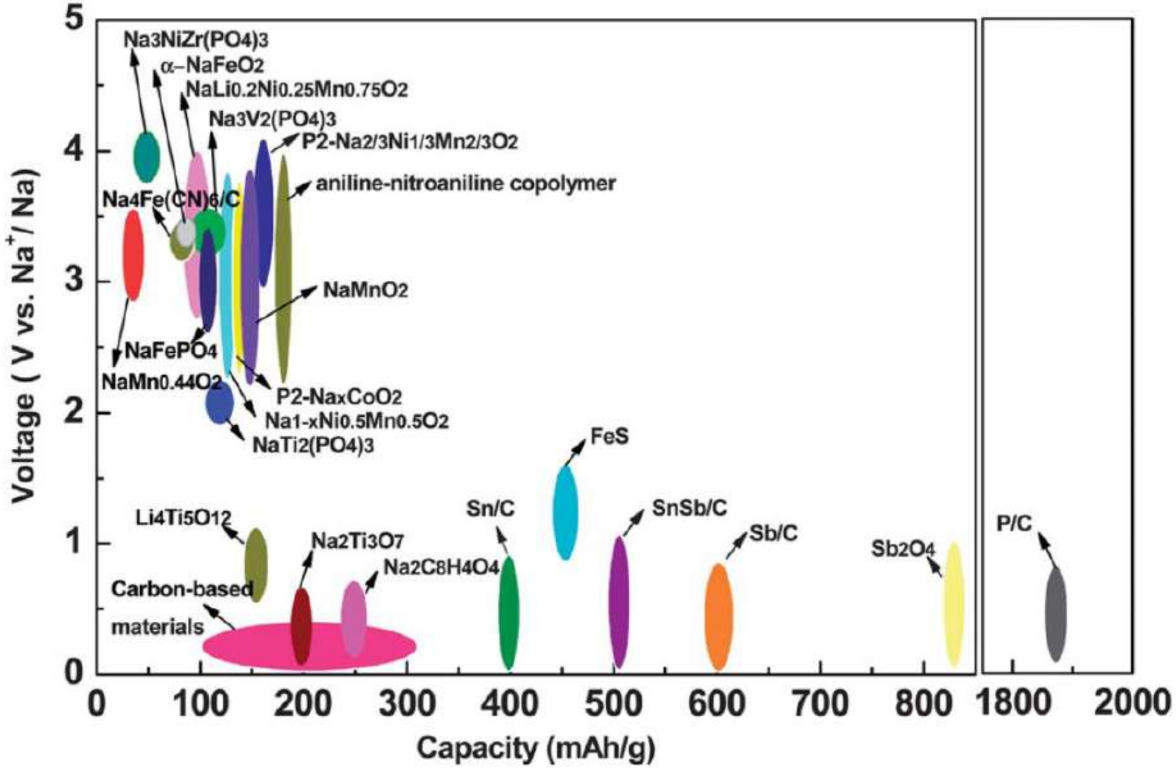

Room-Temperature Stationary Sodium-Ion Batteries for Large-Scale Electric Energy Storage
H. Pan, Energy Environ. Sci., 2013, 6, 2338

From Lithium to sodium with liquid based batteries, with glassy and glass ceramic cathodes

controlled crystallization and evolution of variable proportions of crystalline and glassy phases

⇒ glass-ceramics cathodes can significantly outperform conventional crystalline cathodes in terms of

- superior mechanical properties,
  - good formability,
  - strong electrochemical stability,
- high ionic and electronic conductivity, and chemical resistance to volumetric changes upon dissolution of alkali metal cation

Comparison of the electrochemical performance of glass and glass ceramic cathode materials to the mainstream cathode

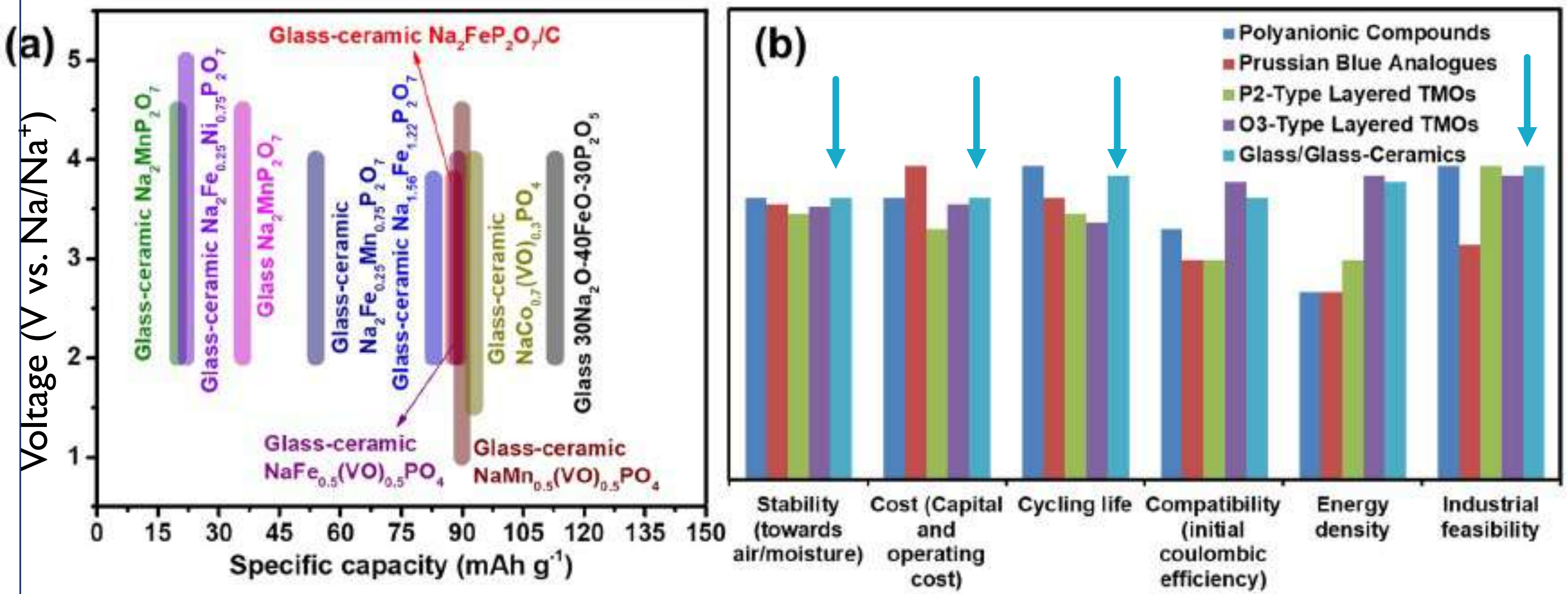

Excellent operating potential of glass and glass-ceramic compounds results in high energy density and specific capacity as well as strong compatibility with the anode due to the high operational potential of the materials.

S. Gandi et al., Journal of Power Sources 521 (2022) 230930

From Lithium to sodium with liquid based batteries, with glassy and glass ceramic cathodes

General tactics for enhancing the performance of glass and glass-ceramic cathode materials

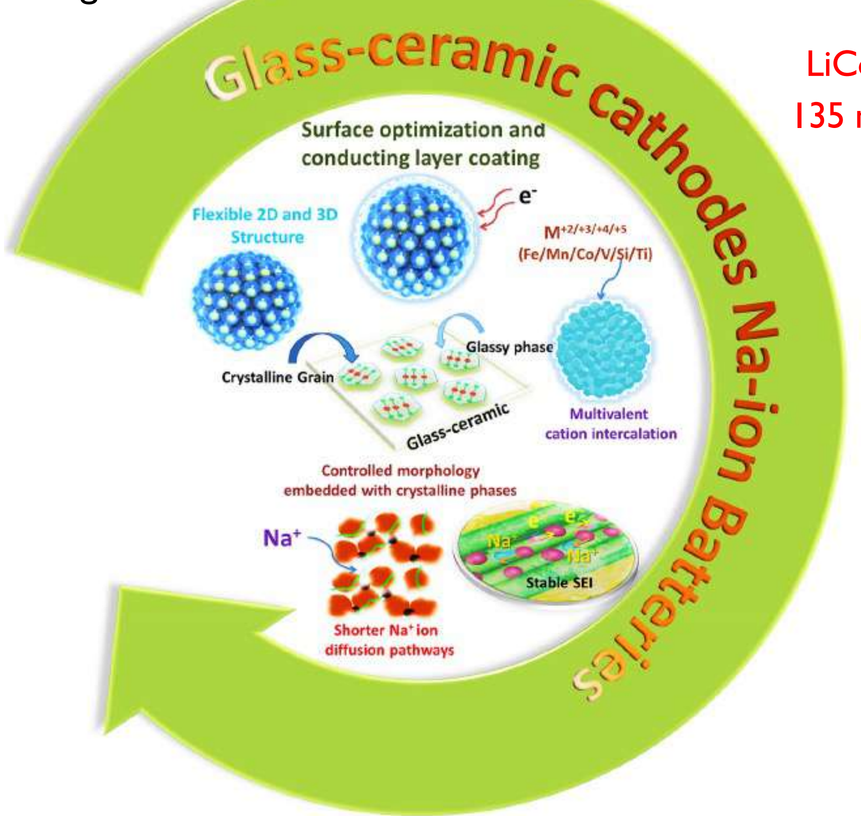

$LiCoO_2$
135 mAh.g⁻¹

glass and glass-ceramic cathode materials tested in SIBs

Glass

	$30Na_2O–40FeO–30P_2O_5$	113 mAh.g⁻¹
	$Na_2MnP_2O_7$	36 mAh.g⁻¹

Glass-ceramic

Pyrophosphate	$Na_2FeP_2O_7/C$	88 mAh.g⁻¹
	$Na_2MnP_2O_7$	20 mAh.g⁻¹
	$Na_2Fe_{0.25}Mn_{0.75}P_2O_7$	54 mAh.g⁻¹
	$Na_2Fe_{0.25}Ni_{0.75}P_2O_7$	22 mAh.g⁻¹
Mixed polyanion	$NaFe_{0.5}(VO)_{0.5}PO_4$	89 mAh.g⁻¹
	$NaMn_{0.5}(VO)_{0.5}PO_4$	90 mAh.g⁻¹
	$NaCo_{0.7}(VO)_{0.3}PO_4$	93 mAh.g⁻¹

prepared melt quenching method and heat-treated at crystalline temperature to produce glass ceramics

S. Gandi et al., Journal of Power Sources 521 (2022) 230930

Na ion conductors

- β-alumina (consisting of β and β″ phases) and a NASICON-type crystal (Ceramatec) have a higher conductivity of 10^{-3} S cm^{-1} at RT but sintering at a high temperature of 1,800 °C needed to reduce the grain-boundary resistance for β-alumina.
- Conductivity of the Na_3PS_4 glass-ceramic electrolyte one order of magnitude lower than that of sintered β-alumina and the NASICON-type crystal but good electrode–electrolyte contact by simple cold pressing.
- Na_3PS_4 glass-ceramic exhibits higher conductivity than sulfide glasses and a $Na_3Zr_2Si_2PO_{12}$ NASICON crystal.

Conductivities of several Na^+ ion conductors

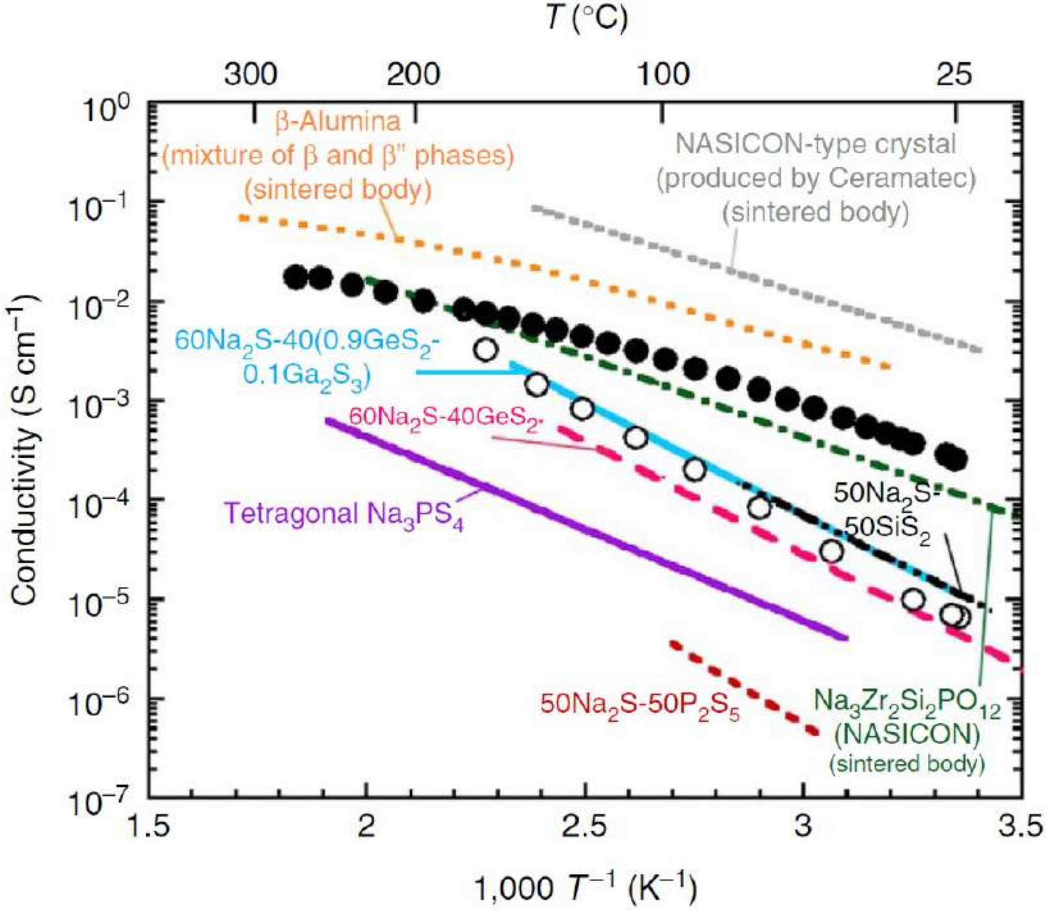

Na_3PS_4 glass-ceramic prepared at 270 °C (●)

Na_3PS_4 glass (○)

A. Hayashi, K. Noi, A. Sakuda, M. Tatsumisago, Nature Communications 3 (2012) Article number: 856, 1-5.

All-Solid-State Batteries with oxide electrolyte

$Na_2FeP_2O_7$ GC //, beta'' -alumina SE //Na metal
pressureless cofiring at 550 °C

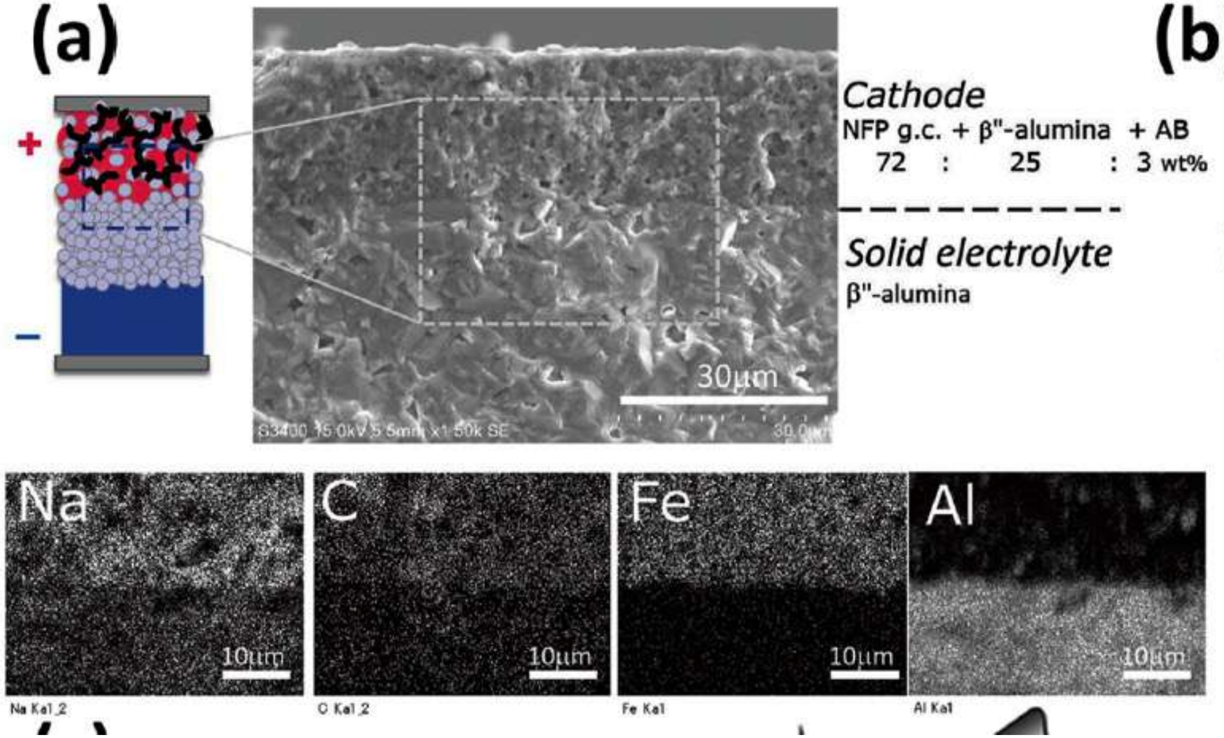

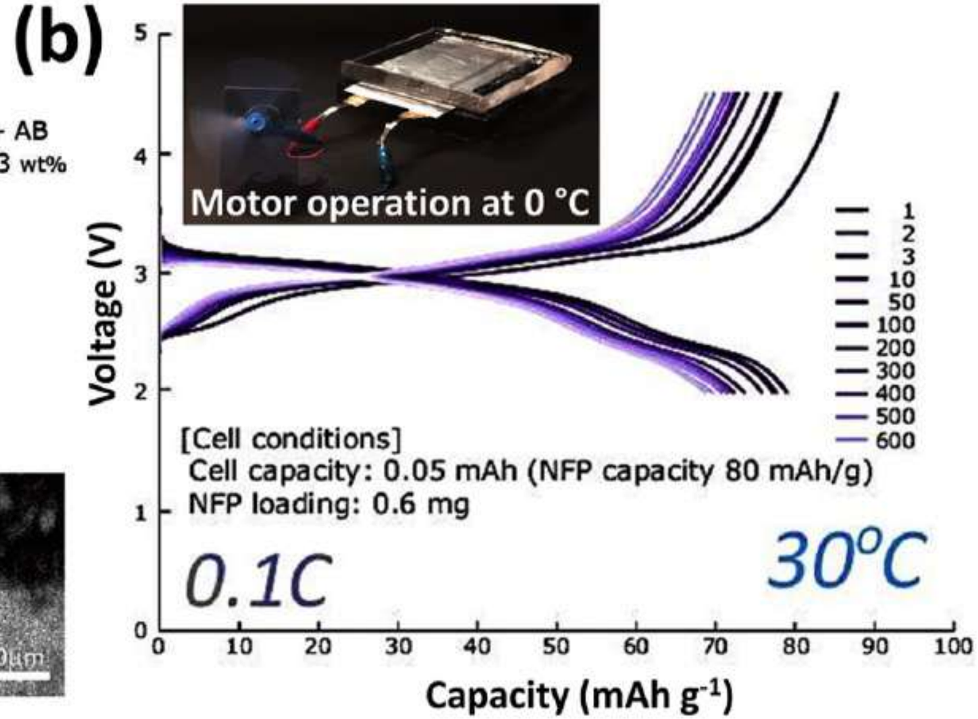

quick charge and discharge capabilities that can operate not only at room temperature (30 °C) but also at -20 °C.

All-Solid-State Batteries with sulfide electrolyte

Glass (ball-milling)

Glass Ceramic 270 °C cubic

Glass Ceramic 420 °C tetragonal

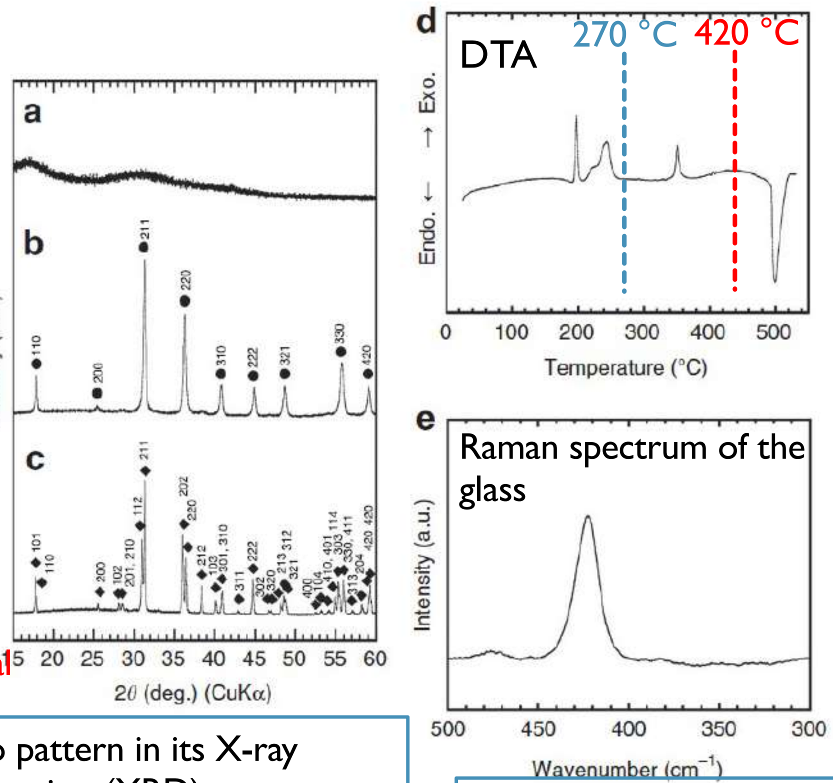

halo pattern in its X-ray diffraction (XRD) pattern

single band at 420 cm⁻¹,
⇒ ortho-thiophosphate ion (PS_4^{3-})

A. Hayashi, K. Noi, A. Sakuda, M. Tatsumisago,
Nature Communications 3 (2012) Article number: 856, 1-5.

Crystal structure of Na_3PS_4 projected in the (010) plane

Cubic
High-temperature phase

Tetragonal
Low-temperature phase

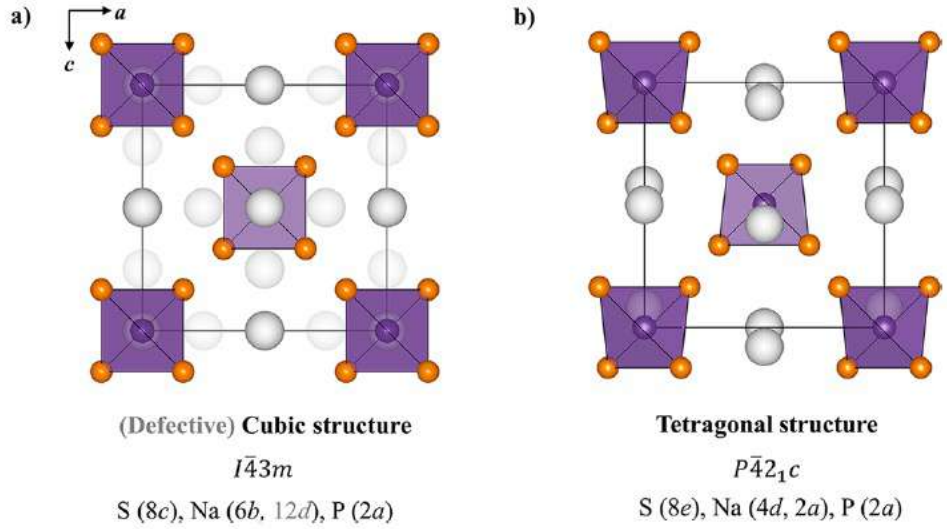

- No occupancy of the 12d positions)
- PS_4^{3-} tetrahedra in a body centered lattice.

- minor rotation of the tetrahedra
⇒ splitting of the Na positions
⇒ elongation of the c-lattice parameter.

T. Krauskopf, Inorg. Chem. 2018, 57, 4739−4744

All-Solid-State Batteries with sulfide electrolyte

Impedance plots

GC cubic
$\sigma_{ion} = 2\times10^{-4}$ S cm^{-1}
E_a = 27 kJ mol^{-1}

GC Tetragonal
$\sigma_{ion} = 1\times10^{-6}$ S cm^{-1}

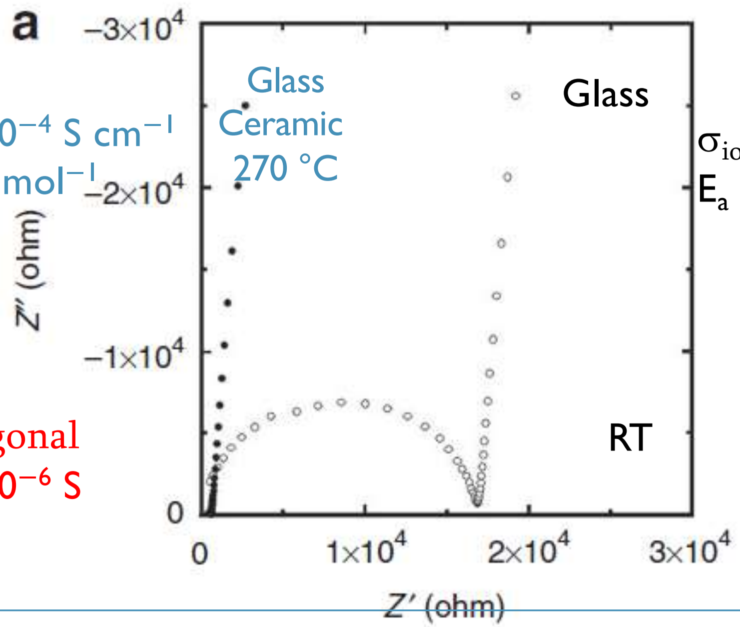

$\sigma_{ion} = 6\times10^{-6}$ S cm^{-1}
E_a = 47 kJ mol^{-1}

Glass: semicircle and a spike in the low-frequency region
⇒ typical ionic conductor.
⇒ total conductivity includes the bulk-grain and grain-boundary resistances
Glass-ceramic: resistance of the pellet decreases by a factor of 30 on crystallization

Cross-sectional SEM images

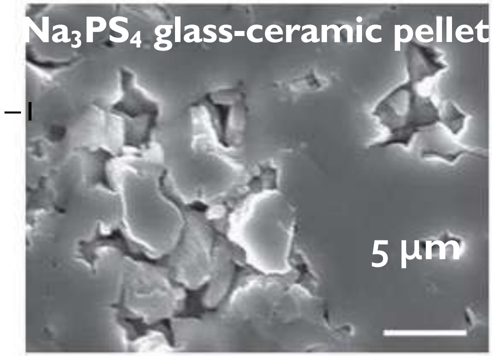

Intimate contacts among particles achieved in the Na_3PS_4 glass-ceramic pellet

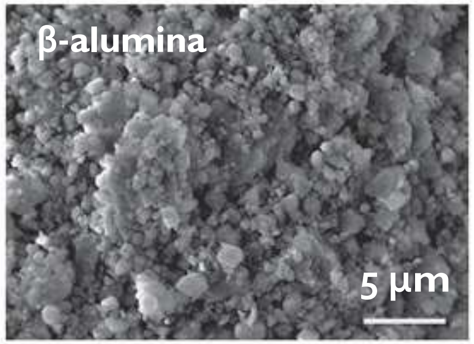

Grain-boundaries among particles clearly observed in the β-alumina pellet

A. Hayashi, Nature Communications 3 (2012) Article number: 856, 1-5.

Na ion conductors

Cathode composite

Chevrel phase Mo_6S_8 ~1.4 V (vs Na/Na^+)
coated with a thin layer of Na_3PS_4
+ Na_3PS_4 glass-ceramic
+ Acetylene black

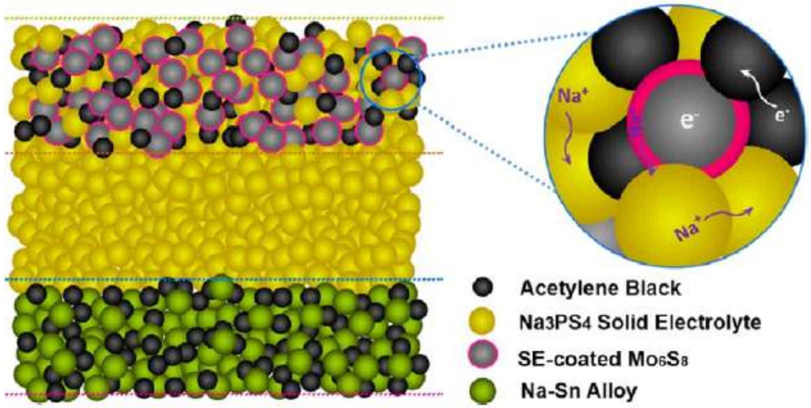

Anode composite

Na-Sn alloy
Acetylene black

Na batteries

Charge−discharge profiles
at various current densities from 5 to 60 $mA.g^{-1}$

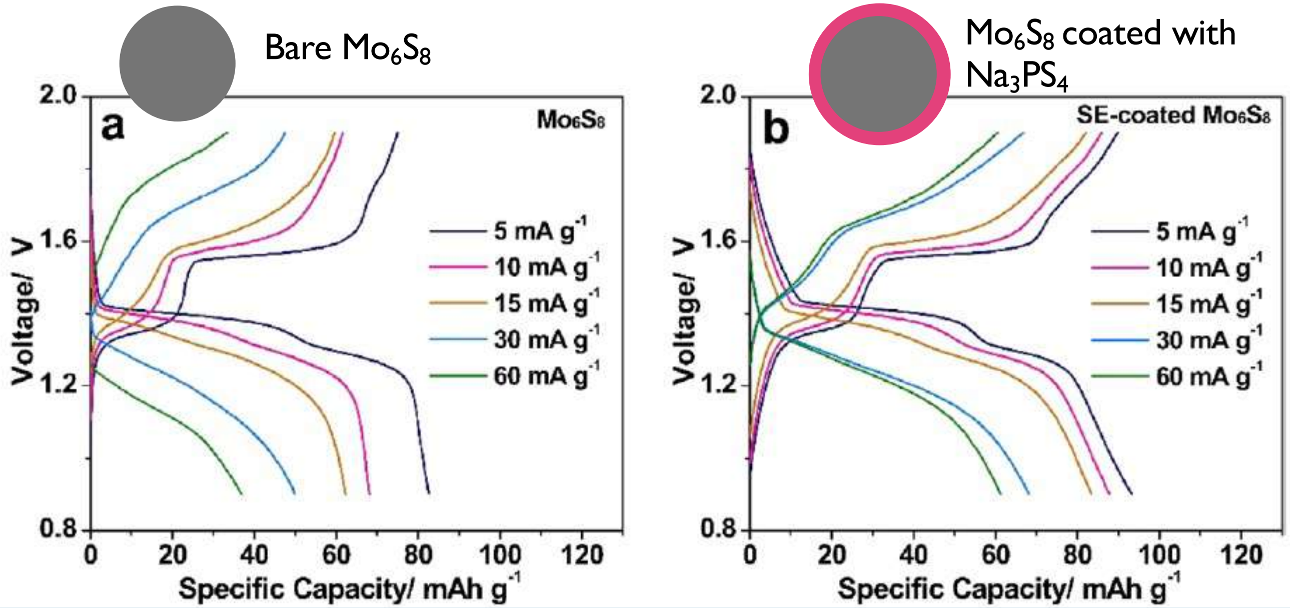

- Decrease of the capacities with increasing currents
- The SE-coated Mo_6S_8 electrode delivers higher capacities than the bare Mo_6S_8 electrode at the same currents.

⇒ Enhanced rate performance of SE-coated Mo_6S_8

Long Cycle Life All-Solid-State Sodium Ion Battery
J.Yue, ACS Appl. Mater. Interfaces 2018, 10, 39645−39650

Na ion conductors

Na batteries

Cycling performances and Coulombic efficiencies of the Mo_6S_8 and SE-coated Mo_6S_8 cathodes in ASIBs at 60 mA.g^{-1} at 60 °C.

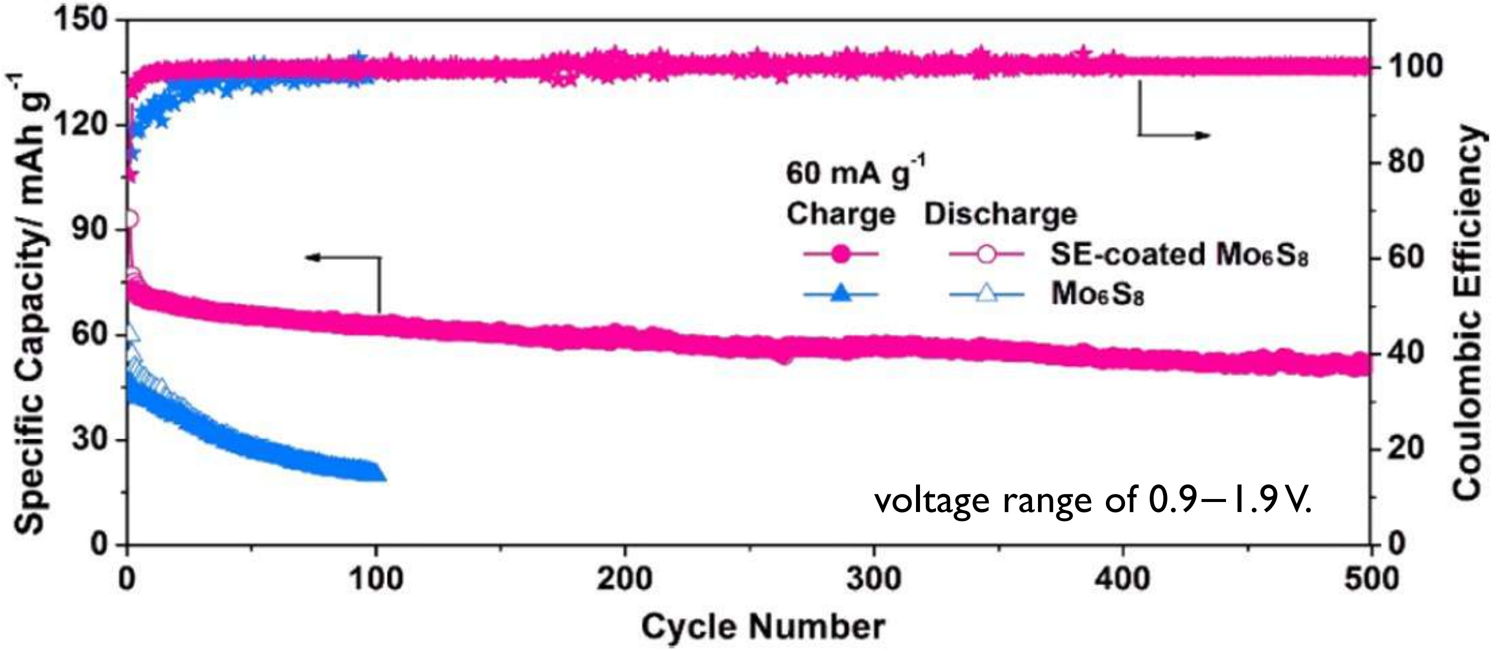

- Limited potential (voltage range of 0.9–1.9 V) but high cycling performance (500 cycles)
- Thin layer of Na_3PS_4 coated on Mo_6S_8 ⇒ solution method to achieve an intimate contact between Mo_6S_8 and the SE

Long Cycle Life All-Solid-State Sodium Ion Battery
J. Yue, ACS Appl. Mater. Interfaces 2018, 10, 39645–39650

4

Conclusions and perspectives

Reduce CO_2 emission
Energy storage from renewable energie

Batteries

Limitation of traditional Li-Ion batteries

All-Solid-State batteries Li-Ion batteries
Li metal (3860 mAh g^{-1})
Solid state electrolyte:
wider potential window: High potential material
Higher energy density
Safety

Solid electrolytes: glass, glass ceramics and crystalline phases

Oxides

Sulfides

All-Solid-State Batteries

No glass used in All-Solid-State Batteries
Only Glass-ceramic

Glass and glass-ceramic solid electrolytes

New synthetic routes since the 2000s

thermal-image furnace
and twin roller

Melting
+ quenching

oxides

Ball-milling

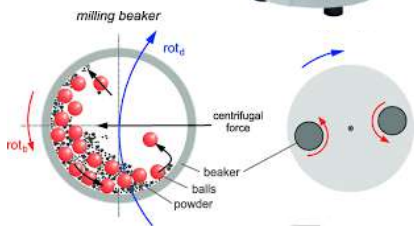

Solvent assisted synthesis

sulfides

- Glass-ceramics
  - 80-20 Li_2S-P_2S_5
  - 70-30 Li_2S-P_2S_5
  - $Li_7P_3S_{11}$
- Superionic conductive crystal
  - $Li_7P_3S_{11}$
  - Na_3PS_4
- Stable crystalline phase with lower Grain-Boundary resistance
  - LATP
  - LAGP

- Air stability and Li metal compatibility in sulfide based solid electrolytes
  - P substitution by Sn, Sb and Zn
  - S substitution by O

Challenges for the ASSB assembling

Large choice of active materials

Different technologies
- **Na**
- **Li**
- **(Li-S)**

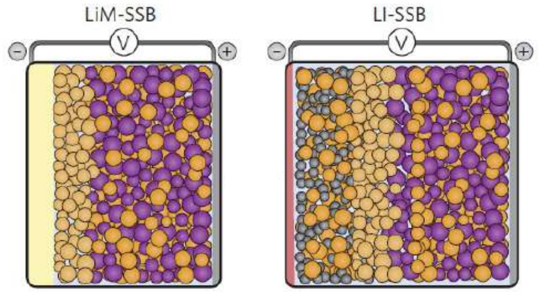

Cycling possible at high temperature

Strategies to improve interface (coating)

Machine learning (coating, formulation, electrolyte)

Poster 12 (Sajid Mannan) - Deciphering Glass Dissolution Rates: A Machine Learning Perspective for Prediction and Interpretation

Assembling processes

powder pressing process

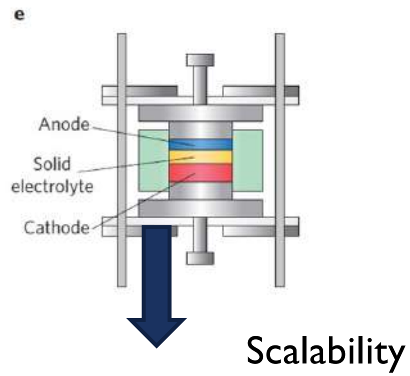

Solution processed

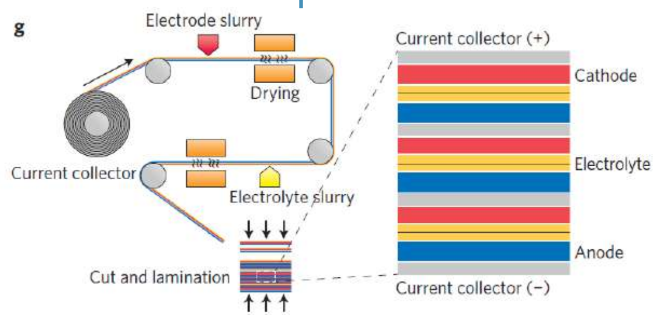

Bibliography

In addition to the references already given at the bottom of the slide

Emerging Role of Non-crystalline Electrolytes in Solid-State Battery Research
Zane A. Grady *et al*,. *Frontiers in Energy Research* 8 (2020): 218

Towards Higher Electric Conductivity and Wider Phase Stability Range via Nanostructured Glass-Ceramics Processing
Tomasz K. Pietrzak *et al*., *Nanomaterials-Basel*. 11 (2021) 1321

Inorganic sodium solid-state electrolyte and interface with sodium metal for room-temperature metal solid-state batteries
Jin An Sam Oh *et al*., *Energy Storage Materials* 34 (2021): 28-44.

Interfaces and Interphases in All-Solid-State Batteries with Inorganic Solid Electrolytes
Abhik Banerjee *et al*., *Chemical reviews* 120.14 (2020): 6878-6933.

Progress and perspective of glass-ceramic solid-state electrolytes for lithium batteries.
Liyang Lin *et al*., *Materials* 16.7 (2023): 2655.

Recent progress in the development of glass and glass-ceramic cathode/solid electrolyte materials for next-generation high capacity all-solid-state sodium-ion batteries: A review.
Suman Gandi *et al*., *Journal of Power Sources* 521 (2022): 230930.

GLASS (AND GLASS CERAMICS) FOR BATTERIES

Acknowledgements

Vincent Seznec

OSAKA UNIVERSITY

Masahiro Tatsumisago
Hayashi Akitoshi

Institut Charles Gerhardt Montpellier

Annie Pradel
Andrea Piarristeguy

International Commission on Glass

Thanks for your attention